



**NTNU – Trondheim**  
Norwegian University of  
Science and Technology

# Modelling of Loads and Responses of a Permaskirt on a Flexible Net Cage Fish Farm

**Ole Alexander Stavnem**

Marine Technology (2-year)  
Submission date: June 2014  
Supervisor: Sverre Steen, IMT

Norwegian University of Science and Technology  
Department of Marine Technology





## **MASTER THESIS IN MARINE TECHNOLOGY**

**SPRING 2014**

**FOR**

**Ole Stavnem**

### **Modelling of loads and responses of a Permaskirt on a flexible net cage fish farm**

To reduce the number of laryngic salmon louse entering the fish farms, it is proposed to cover the upper part of the net cage with a watertight fabric skirt. However, this will significantly change the hydrodynamic loads on the net cage, especially from current. The simulation tool Aquasim is currently in widespread use in engineering calculations of fish farms. However, this tool doesn't currently have the capability to include such skirts in the simulation. In addition, it is of interest to know more about the effectiveness of such a skirt in stopping the laryngic salmon louse to enter the net cage. Since the larvae is drifting with the current close to the surface, the effectiveness of the skirt can be measured in terms of the two-dimensionality of the flow around the skirt.

Therefore, the objectives of the master thesis are:

- To develop a model for the loads on the skirt in aquasim
- To investigate the effectiveness of the skirt in keeping the larvae out of the net cage.

In the thesis the candidate shall present his personal contribution to the resolution of problem within the scope of the thesis work.

Theories and conclusions should be based on mathematical derivations and/or logic reasoning identifying the various steps in the deduction.

The thesis work shall be based on the current state of knowledge in the field of study. The current state of knowledge should be established through a thorough literature study, the results of this study shall be written into the thesis. The candidate should utilize the existing possibilities for obtaining relevant literature.

The thesis should be organized in a rational manner to give a clear exposition of results, assessments, and conclusions. The text should be brief and to the point, with a clear language. Telegraphic language should be avoided.

The thesis shall contain the following elements: A text defining the scope, preface, list of contents, summary, main body of thesis, conclusions with recommendations for further work, list of symbols and acronyms, reference and (optional) appendices. All figures, tables and equations shall be numerated.

The supervisor may require that the candidate, in an early stage of the work, present a written plan for the completion of the work. The plan should include a budget for the use of computer and laboratory resources that will be charged to the department. Overruns shall be reported to the supervisor.



**NTNU Trondheim**  
**Norwegian University of Science and Technology**  
*Department of Marine Technology*

The original contribution of the candidate and material taken from other sources shall be clearly defined. Work from other sources shall be properly referenced using an acknowledged referencing system.

The thesis shall be submitted electronically (pdf) in DAIM:

- Signed by the candidate
- The text defining the scope (signed by the supervisor) included
- Computer code, input files, videos and other electronic appendages can be uploaded in a zip-file in DAIM. Any electronic appendages shall be listed in the main thesis.

The candidate will receive a printed copy of the thesis.

Supervisor : Professor Sverre Steen  
Advisor : Line Heimstad  
Start : 14.01.2014  
Deadline : 10.06.2014

Trondheim, 14.01.2014

Sverre Steen  
Supervisor

## Abstract

As the numbers of fish farms are increasing, the problems with lice are becoming of greater importance. The lice cause diseases and death, leading to loss in profit for the fish farms as well as reduction of the wild stock. To deal with this problem, many solutions have been introduced. For example, placing the fish farms on land or make the fish farms as floating concrete structures. However, these suggestions are costly.

Another idea is to put a watertight skirt, a Permaskirt, around the upper part of the net cage. However, the introduction of such a skirt would increase the loads and responses on the structure. This thesis shows how to calculate these forces and displacements, and how they are increased when a watertight skirt is placed around the net cage, by using the finite element analysis software AquaSim by Aquastructures.

The program is used to calculate the drag and net displacements when current forces influence the structure. Results are compared to results from model experiments and calculations done by the program FhSim.

The introduction of such a skirt will also influence the pressure and flow distribution around the net cage. An investigation regarding the flow distribution, to see if the flow travels under the skirt, will therefore be of importance to evaluate the effect of Permaskirt. In order to investigate these effects, computational fluid dynamic (CFD) calculations has been performed, using the Ansys software.

The analysis shows that the AquaSim program overestimates the forces and displacements, compared with experimental values. Possible solutions to obtain correct calculations in AquaSim, by using varying solidity for the skirt, has been presented and shows good results compared with experimental values.

CFD analysis shows that a skirt covering the upper part of a net cage would reduce 99.61% of the water particles, from the upper part of the water layer, to enter the upper part of the net cage, leading to reduction of lice contamination on the fish in the net cage.

This page is intentionally left blank.

## Sammendrag

Ettersom antall oppdrettsanlegg stadig øker, blir det stadig viktigere å hensyn til lakselus problematikken. Lakselusen fører til sykdommer og død, som gir redusert lønnsomhet for oppdrettsanleggene samt reduksjon av den norske villaks stammen. For å løse dette problemet, har flere metoder blitt introdusert. Metoder som oppdrettsanlegg på land, eller nøter av betong har blitt introdusert, men disse metodene er dyre.

En annen idé er å plassere en vanntett duk, kalt for Permaskjørt, rundt øvre del av noten. Dette vil være en billigere metode, men krefter og deformasjoner på konstruksjonen vil øke. Denne oppgaven viser hvordan man kan regne ut disse kreftene og deformasjonene, samt hvor mye de vil øke om et skjørt blir plassert rundt noten. For å kunne regne ut dette har simuleringsprogrammet AquaSim, utviklet av Aquastructures, blitt brukt.

Programmet er brukt til å regne ut krefter og deformasjonen når strøm påvirker noten. Resultatene er sammenlignet med resultater fra forsøk og simuleringer gjort av programmet FhSim.

Montering av skjørt på en not vil også påvirke trykk og strømningsbildet rundt noten. Undersøkelse av strømningsbildet, for å se om noe av vannet blir presset under skjørtekanten vil være viktig for å kunne evaluere effekten av Permaskjørt. For å kunne undersøke disse effektene har ”computational fluid dynamic” (CFD) blitt utført ved å bruke programmet Ansys.

Analysene viser at AquaSim overestimerer både krefter og deformasjon sammenlignet med eksperimentelle data. Mulige løsninger for å kunne simulere krefter og deformasjon korrekt, ved å bruke lokal soliditet på skjørtet, har blitt presentert og gir gode resultater sammenlignet med eksperimentelle verdier.

CFD analyser viser at et skjørt som dekker øvre del av noten vil redusere 99.61% av vannpartiklene fra øvre vannlag fra å komme inn under skjørtet, som vil gi reduksjon i lusepåslag på fisk i noten.

This page is intentionally left blank.



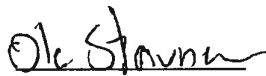
### Acknowledgements

In association with the work done writing this Master thesis, there are people I would like to thank. Their help and support throughout this process has been very valuable.

First of all I will direct my gratitude to my supervisor Sverre Steen. His general advices and support is much appreciated.

I would also like to thank Aquastructures, for giving me the opportunity for working with this topic. Line Heimstad, thank you for answering all my e-mails. It was of great help.

Lastly I would like to thank Per Rundtop and Andreas Lien from SINTEF for providing the data from the experiment in Hirtshals.



Ole Stavnem

Trondheim, June 6, 2014

This page is intentionally left blank.

# Contents

<b>1</b>	<b>Introduction</b>	<b>1</b>
1.1	Background and motivation . . . . .	1
1.2	Background on net cages . . . . .	2
1.3	NS 9415 . . . . .	4
1.4	Previous work . . . . .	5
1.5	Previous calculation methods . . . . .	7
1.5.1	Projected area method . . . . .	7
1.5.2	Potential flow theory . . . . .	8
1.5.3	Forces on a three dimensional net cage . . . . .	9
1.6	FhSim simulation . . . . .	10
1.7	Load formulation in AquaSim . . . . .	10
1.7.1	Reduced velocity. . . . .	12
1.7.2	Finite element analysis . . . . .	13
1.8	CFD analysis . . . . .	14
<b>2</b>	<b>Modelling methods</b>	<b>15</b>
2.1	Potential flow theory . . . . .	15
2.2	Model testing of a net cage with Permaskirt . . . . .	15
2.3	The AquaSim software package. . . . .	16
2.3.1	AquaSim modelling . . . . .	17
2.4	Ansys CFD . . . . .	22
2.4.1	Ansys modelling . . . . .	22
<b>3</b>	<b>Results and discussion</b>	<b>26</b>
3.1	Pressure distribution . . . . .	26
3.2	AquaSim results . . . . .	27
3.2.1	Reduced velocity . . . . .	28
3.2.2	Full configuration . . . . .	29
3.2.3	Skirt only . . . . .	34
3.2.4	Locally varying solidity . . . . .	36

---

3.3	CFD results . . . . .	43
3.3.1	Pressure distribution . . . . .	43
3.3.2	Velocity distribution . . . . .	44
3.3.3	Comparison with measured data . . . . .	47
3.3.4	Estimated effect of PermaSkirt, based on CFD analysis . . . . .	51
3.3.5	Increased depth . . . . .	53
3.4	Error sources . . . . .	55
3.4.1	Deformation measurement . . . . .	56
3.4.2	CFD modelling . . . . .	57
<b>4</b>	<b>Conclusion</b>	<b>58</b>
4.1	Conclusion . . . . .	58
4.2	Recommendations for further work . . . . .	59
	<b>Bibliography</b>	<b>61</b>
	<b>Appendices</b>	<b>I</b>
<b>A</b>	<b>Simulation results</b>	<b>I</b>

# List of Figures

1.1	Traditional knotted mesh with diamond orientation (left), and knotless mesh with square orientation (right). Courtesy: [Fredheim, 2005]. . . . .	3
1.2	Skirt deformation as seen from the right. Current velocity is 0 <i>m/s</i> (left) and 0.2 <i>m/s</i> (right). It is observed how the net cage will be pushed backwards and get lifted as it is influenced by the current (right). . . . .	3
1.3	Markings of some of the stagnation points on a skirt in a two dimensional plane, seen from above. In this figure, the current travels in the negative x-direction. . . . .	8
1.4	Drag coefficient, $Cd_{cyl}$ , as a function of Reynolds number. Courtesy: [Sumer and Fredsøe, 2006]. . . . .	12
2.1	Key dimensions for the net cage. A skirt depth of 363 <i>mm</i> was used for this thesis. Courtesy: [Lien and Volent, 2012]. . . . .	17
2.2	The fish cage as modeled in AquaEdit. . . . .	18
2.3	Model M2 as modelled in Ansys, seen from the left. The deformation had to be simplified due to complex geometry. . . . .	23
2.4	Meshing for the fluid domain in the simulation. . . . .	23
2.5	Velocity measurements for different mesh sizes used for checking mesh refinement. . . . .	24
3.1	Dynamic pressure distribution on the net, calculated by potential flow theory in Matlab. . . . .	26
3.2	Dynamic pressure distribution calculated by potential flow theory, CFD and AquaSim. . . . .	27
3.3	Drag force, with and without reduced velocity enabled in AquaSim. All results from skirt only configuration. . . . .	28
3.4	Drag force on the net cage, fitted with Permaskirt. Comparison between AquaSim, FhSim and experimental values. All for $Sn=1$ , which implies a watertight skirt. . . . .	29

3.5	Deformation on the fore part of the skirt, for the case with both net cage and Permaskirt. Comparison between AquaSim, FhSim and experimental values. All for $S_n=1$ , which implies a watertight skirt. . . . .	30
3.6	Deformation on the aft part of the skirt, for the case with both net cage and Permaskirt. Comparison between AquaSim, FhSim and experimental values. All for $S_n=1$ , which implies a watertight skirt. . . . .	31
3.7	Drag force on the net cage, fitted with Permaskirt. $S_n = 0.9$ to $0.6$ indicates the varying solidity in AquaSim. Both FhSim calculation and experimental test values was obtained with $S_n=1$ . . . . .	32
3.8	Deformation on the fore part of the skirt attached to the net cage. $S_n = 0.9$ to $0.6$ indicates the varying solidity in AquaSim. Both FhSim calculation and experimental test values was obtained with $S_n=1$ . . . . .	32
3.9	Deformation on the aft part of the skirt attached to the net cage. $S_n = 0.9$ to $0.6$ indicates the varying solidity in AquaSim. Both FhSim calculation and experimental test values was obtained with $S_n=1$ . . . . .	33
3.10	Drag force on the structure, with Permaskirt only. $S_n = 0.9$ to $0.6$ indicates the varying solidity in AquaSim. Both FhSim calculation and experimental test values was obtained with $S_n=1$ . . . . .	34
3.11	Deformation on the fore part of the skirt, for the case with skirt only. $S_n = 0.9$ to $0.6$ indicates the varying solidity in AquaSim. Both FhSim calculation and experimental test values was obtained with $S_n=1$ . . . . .	35
3.12	Deformation on the fore part of the skirt, for the case with skirt only. $S_n = 0.9$ to $0.6$ indicates the varying solidity in AquaSim. Both FhSim calculation and experimental test values was obtained with $S_n=1$ . . . . .	36
3.13	Drag force on the construction with only the skirt attached to the floating tubes. " $S_n = 0.7$ " indicates the case with a uniform solidity of $0.7$ calculated in AquaSim. "Experiment" is the values obtained in Hirtshals, and "Varying solidity" indicates the case discussed in this chapter. . . . .	37
3.14	Deformation on the fore part of the skirt. " $S_n = 0.7$ " indicates the case with a uniform solidity of $0.7$ calculated in AquaSim. "Experiment" is the values obtained in Hirtshals, and "Varying solidity" indicates the case discussed in this chapter. . . . .	38
3.15	Deformation on the aft part of the skirt. " $S_n = 0.7$ " indicates the case with a uniform solidity of $0.7$ calculated in AquaSim. "Experiment" is the values obtained in Hirtshals, and "Varying solidity" indicates the case discussed in this chapter. . . . .	39
3.16	Drag force computed by AquaSim, compared with calculations executed by FhSim and experimental data. AquaSim had full net cage configuration with locally varying solidity for the skirt. . . . .	40

3.17	Deformation at the fore side of the skirt. AquaSim had full net cage configuration with locally varying solidity for the skirt. . . . .	41
3.18	Deformation at the aft side of the skirt. AquaSim had full net cage configuration with locally varying solidity for the skirt. . . . .	41
3.19	Pressure distribution on the deformed skirt, seen from the left, at $U = 0.1m/s$ . Maximum pressure is 5.38 Pa and minimum is -4.43 Pa. . . . .	43
3.20	Contour plot of the velocity distribution at the free surface. The velocity is in $m/s$ . . . . .	44
3.21	Vector plot of the velocity distribution at the free surface. Note that the water inside of the skirt travels in opposite direction of the undisturbed current. The colorbar is difficult to read, but it is the same as for figure 3.20. . . . .	45
3.22	Contour plot of the velocity distribution in the vertical plane. . . . .	46
3.23	Vector plot of the velocity distribution in the vertical plane. . . . .	47
3.24	Placement of electromagnetic velocity sensors in the experiment. Green box indicates load cell for drag force, while red crosses indicates velocity sensors. Courtesy: [Lien and Volent, 2012]. . . . .	48
3.25	Comparison of flow velocity and direction between CFD simulation and experiment for five different positions. Blue dots indicate direction [deg] and thin red line indicates magnitude of current [ $cm/s$ ] in the experiment. Thick red line indicates simulated current velocity and thick black line indicates simulated direction. 0 degrees indicates free current direction, while 180 degrees indicates velocity against the undisturbed current. . . . .	49
3.26	Isometric view of the streamlines used for calculating the number of particles entering the volume limited by the skirt. For this case, 2/1000 of the streamlines projected from the plane in front of the skirt were circulated inside the skirts volume. . . . .	51
3.27	Flow distribution, displayed as path lines with a tank depth of 5.4m. Color bar shows the velocity in $m/s$ . . . . .	53
3.28	Current velocity as a function of depth. The velocity distribution is presented 5 meters in front of the skirt, 5 meters behind the skirt and at the center. . . . .	54
3.29	Current velocity as a function of depth with increased water depth. The velocity distribution is presented 5 meters in front of the skirt, 5 meters behind the skirt and at the center. . . . .	55
3.30	Isometric view of the skirt deformation in AquaSim. . . . .	56
A.1	Results from drag force [N] simulation in AquaSim, presented as numbers. . . . .	I
A.2	Results from deformation simulation at the fore side of the skirt, presented as percent of initial skirt depth. . . . .	II

A.3	Results from deformation simulation at the fore side of the skirt, presented as percent of initial skirt depth. . . . .	III
A.4	Drag force values for net cage only. The net cage had a solidity of 0.21. . .	IV



# List of Tables

2.1	Full scale dimensions of the investigated net cage. . . . .	19
2.2	Multiplication factors used for scaling to model size. $\lambda = 17$ . . . . .	19
2.3	Scaled net cage dimensions used in the experiment and AquaSim simulations. . . . .	19
2.4	Properties for the floating tubes in AquaSim. . . . .	20
2.5	Properties for the sinker tube in AquaSim. . . . .	20
2.6	Properties for the net in AquaSim. . . . .	21
2.7	Properties for the mooring line in AquaSim. . . . .	21

## **List of Acronyms**

**3D** Three dimensional

**Deg** Degrees

**CFD** Computational Fluid Dynamics

**DOF** Degrees of freedom

**ext** External

**FEA** Finite element analysis

**FEM** Finite element method

**int** Internal

**M1** CFD model without deformation

**M2** CFD model with deformation

**NTNU** Norwegian University of Science and Technology

**NTNF** Norges Teknisk-Naturvitenskapelige Forskningsråd

**RAS** Reynolds-averaged Navier-Stokes

## Nomenclature

Nomenclature for this thesis. Some of the constants may have different meanings. The explanation will then be given in the text.

$\Delta l$  Distance

$\delta$  Boundary layer thickness

$\theta$  Angle

$\lambda$  Scaling factor of 17

$\lambda_2$  Scaling factor of 15.625

$\rho$  Density of water

$\phi$  Velocity potential

$\nu$  Viscosity

$A$  Area

$A_p$  Projected area

$Cd$  Drag coefficient

$Cd_{cyl}$  Drag coefficient for a cylinder

$Cd_{net}$  Drag coefficient for a net

$D$  Diameter

$d$  Twine diameter

$F$  Force

$F_c$  Drag force on cylinder

$F_n$  Force in the normal direction

$F_t$  Force in the transverse direction

$F_s$  Drag force on sphere

- 
- $F_x$  Force in x-direction
- $F_y$  Force in y-direction
- $g$  Acceleration of gravity
- $h$  Depth of net cage
- $k$  Stiffness coefficient
- $L$  Length
- $L_y$  Twine length between knots in y-direction
- $L_z$  Twine length between knots in z-direction
- $m$  meter
- $p$  Pressure
- $p_o$  Ambient pressure
- $Rn$  Reynolds number
- $r_r$  Reduction factor
- $Sn$  Solidity
- $Sn_{kn}$  Solidity for knotted mesh
- $Sn_{2D}$  Simplified solidity
- $s$  second
- $T$  Temperature
- $t$  Time
- $U$  Current velocity
- $U_t$  Tangential velocity
- $U_1$  Current velocity on first succeeding net
- $u$  Current velocity through a net
- $v$  Inflow velocity relative to the twine

$v_m$  Velocity of the mesh

$v_n$  Normal velocity component of  $v$

$v_t$  Transverse velocity component of  $v$

$v_w$  Fluid velocity induced by wave motion

$x$  Direction in the three dimensional coordinate system

$y$  Direction in the three dimensional coordinate system

$z$  Direction in the three dimensional coordinate system

# Chapter 1

## Introduction

### 1.1 Background and motivation

Salmon lice, together with escaping fish, are regarded as the largest challenges within salmon and trout farming. As fish farming is constantly increasing in popularity, more information and solutions are needed in order to control the biological consequences associated with aquaculture.

Escaping fish leads to genetic pollution and spreading of diseases into the wild stock of species. However, fish escaping the net cage is not the only way diseases may spread. Lice floating in and out of the net cage will attach to the wild stock and harms it. This causes two main problems: The first problem is the economic problem for the fish farms. Fish death and treatment cost both time and money. The other problem is that lice spreading to the wild salmon causes the population to decrease. As a sports angler, the task to reduce spreading of lice are therefore also of personal motivation.

To reduce the number of lice entering the fish farms, it is proposed to cover the upper part of the net cage with a watertight fabric skirt, called Permaskirt. The idea behind this is that the lice floats in the upper part of the water, and a skirt covering the upper part of the net cage would reduce the number of lice entering the net cage. However, this will change the loads on the structure, net deformation and flow distribution. It is therefore important to investigate these factors in order to prevent damages on equipment and fish.

If these skirts are to be mounted on fish farms, it is of importance to know how the dynamic responses will change. As described in [Rundtop and Lien, 2013] there are different problems with the introduction of Permaskirt on fish farms. The skirt increases the drag, which increase the forces on the structure.

Other problems are that the skirt may move in such ways that it will not work as

intended. The skirt may be lifted up due to current or propeller wake. As the skirt is lifted, lice may pass below the skirt. How the water flows in and around the net cage is therefore also important to investigate in order to check if the skirt will work as intended.

The loads and responses on a fish farm with Permaskirt may be found by making a model and test it in a tank, but this is both time consuming and costly. It may therefore be preferable to do numeric simulations, either on its own, or in collaboration with model experiments. In this thesis, the simulation tool AquaSim will be used for calculations. AquaSim is a program developed by Aquastructures and is used today on conventional fish farms, making it possible to do mooring analyses without model experiments.

For calculating the flow distribution, computational fluid dynamic (CFD) calculations with the Ansys software package will be performed.

## 1.2 Background on net cages

A net consist of a number of twines knotted together in order to make up a mesh. Both twine diameter and distance between knots may be varied in order to obtain a net for the specific task it is intended for. The net mesh may then be formed into a net cage, which can be used for different purposes in aquaculture, such as trawls and net cages.

For the fish farming industry in Norway, the circular net cages are the most common. Other types of net cages, such as hinged steel and semi exposed fish farms, exist but will not be discussed in this thesis.

The circular net cages get buoyancy by a floating collar, often made of high density polyethylene (HDPE). This collar gives both buoyancy and structural stiffness so the volume of the net cage is not reduced to any large extent when influenced by environmental forces.

Ropes are then attached between the floating collar and to the sinker system at the bottom of the net cage. The sinker system may be a sinker tube or individual weights, giving stiffness to the structure and ensuring minimal volume reduction. The ropes will then form a frame, which the net cage can be attached to.

The net may be made in different ways depending of application.

Figure 1.1 shows two commonly used types of mesh made up by twines, with both diamond and square orientation. Orientation of the net can be used to obtain square or diamond configuration dependent on what is desired. For fish farming, where a constant flow of water through the mesh is important, the square mesh orientation is favored since it is easier to assure a constant mesh opening.

The use of knotted twines gives a larger contribution to the current forces, as it

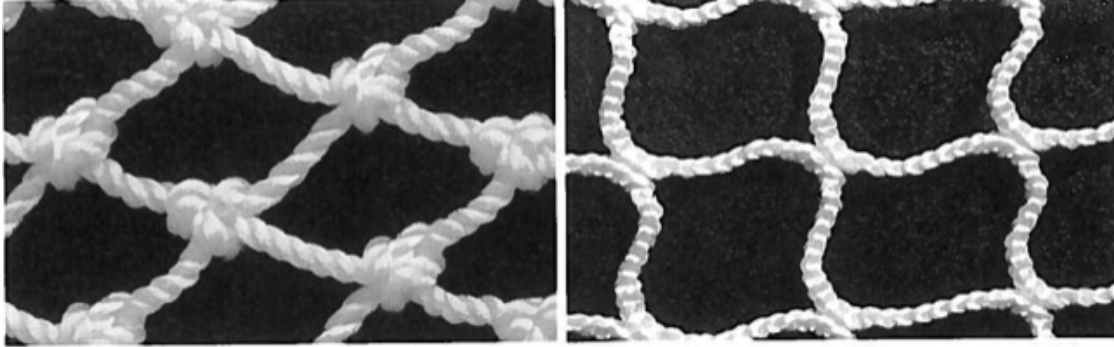


Figure 1.1: Traditional knotted mesh with diamond orientation (left), and knotless mesh with square orientation (right). Courtesy: [Fredheim, 2005].

gives a larger area affected by the current. What kind of mesh type used is therefore important when calculating the forces on the structure. The distance between the knots, an important parameter for the solidity of the net, is also of great influence for the total force on the net structure. The solidity ratio is defined as  $S_n = A_e/A_{tot}$ , where  $A_e$  is the area casting shadow from a light perpendicular to the net and  $A_{tot}$  is the total area of the net [Berstad et al., 2012]. A solidity of 1 will therefore imply a watertight net, such as Permaskirt. Formulas for the solidity ratio, based on twine diameter and length between knots, are presented in equation 1.9 and 1.10.

As most of the fish farms are along the coastline, current and waves are of concern. The net cage has a large area that is greatly influenced by the current. When the current influences the net, it will get pushed back and upwards, reducing the projected area facing the incoming current (fig. 1.2). This deformation is therefore important to include in drag force calculations.



Figure 1.2: Skirt deformation as seen from the right. Current velocity is 0  $m/s$  (left) and 0.2  $m/s$  (right). It is observed how the net cage will be pushed backwards and get lifted as it is influenced by the current (right).



This thesis will look closer into the problems regarding the forces and responses that will occur when a Permaskirt is added to the net cage. As the skirt is watertight, larger forces will influence the net cage, giving larger responses.

### 1.3 NS 9415

NS 9415 was released in 2009 and states the requirement for site survey, risk analysis, design, dimensioning, installation and operations of marine fish farms. It was made in order to reduce the risk of fish escaping due to technical failure or improper use of the equipment. The standard states that all net cages must have its capacity validated through analysis if one or more of the following criteria are met:

- Net depth larger than 40 meters.
- Net circumference larger than 170 meters.
- 50 year wave height larger than 2.5 meters.
- 50 year current velocity larger than 0.75 meters per second.

For the environmental study, wind and current measurements shall be performed before the construction is installed.

Current velocity is measured at 5 and 15 meters under the free surface and is found by one of the three following methods.

- One year measurement and use of long term statistics.
- One month measurement multiplied by a factor found in the standard. This factor depends on the measured values.
- Use of previous measured data if they satisfy the criteria for the previous mentioned methods.

For wave measurement, the waves are split into wind generated waves and swells. Formulas for finding wind generated waves as a function of wind velocity are given together with guidelines in how to use weather data. Swells are not of concern if the site is in sheltered water, but if they appear there are given methods in how to include them in the calculation.

The model examined in this thesis [Lien and Volent, 2012] take base in a 157 meters in circumference net cage with a net depth of 20 meters. Maximal current velocity tested in the model test was  $0.2m/s$ , without any waves. This gives a full scale current velocity of  $0.82m/s$ , and the tested net cage is therefore within the criteria stated by NS 9415.

## 1.4 Previous work

For Permaskirts mounted on net cages, there is not much information to find. There have been done experiments by SINTEF in the flume tank in Hirtshals [Lien and Volent, 2012]. More information about this report is given in chapter 2.2. For this thesis, the experiment is used as comparison for the simulated results.

There has also been written a SINTEF report about the use of the simulation tool FhSim to reproduce the results from the flume tank [Rundtop and Lien, 2013]. FhSim is explained in chapter 1.6. The report is of the same nature as this thesis, since it also tries to calculate the effects of mounting a Permaskirt on a net cage using computer software. It has therefore been of great help in both the modelling and result part of this thesis.

For calculation of drag force and displacement on a regular net without Permaskirt, more information is available.

In 1988 NTN started a three year project about forces on and flow through fish cages. The results are presented in [Løland et al., 1988], [Aarsnes et al., 1989] and [Løland, 1991], where [Løland, 1991] is a PhD thesis. Calculation methods developed in the three year project, such as the project area method in chapter 1.5.1, and the reduced velocity in chapter 1.7.1, has been used in this thesis. The three year project includes different calculation models that are verified against model experiments.

There has also been written articles about calculation of forces and displacements on net and net cages. [Tsukrov et al., 2003] propose a consistent finite element for hydrodynamic response and results are compared with experimental observations. [Lader et al., 2007] describes experiments to investigate forces from waves and current for fish farm in open ocean locations.

[Lader and Enerhaug, 2005] is another report based on experiments. A circular model is placed in a flume tank and tested with different weights in order to find forces and deformations. Dependence between forces and deformation is investigated and presents numerical models for calculation. The numerical models presented in this article are basis for the formulation in AquaSim.

In order to find added mass, [Balash et al., 2009] did an experiment combined with numerical calculations. It took place in both steady and oscillating flow. Still, for this thesis, only the steady flow is of interest.

[Li et al., 2013] developed a buoyancy distribution method in order to find the instantaneous buoyancy of the floater, for this thesis waves are not included and this method has not been considered. In general they all apply different methods to calculate the load and response on net membranes with various degree of interest regarding this thesis.

[Fredheim, 2005] is a PhD thesis performed in order to developed a three-dimensional model for the flow in front and inside a net structure. The developed model is presented

in chapter 1.5.3.

The use of finite element method in order to calculate forces and deformations on a net cage has also been performed. As the Norwegian Standard, NS 9415, was released, new criteria were established. [Berstad et al., 2004] developed the finite element method (FEM) program AquaSim in order to meet these new requirements. By using beam, membrane and bar elements, net cages could be modelled. The calculation methods developed and used in AquaSim are shown in chapter 1.7.

[Moe et al., 2010] also developed a method for structural analysis of net cages using finite element analysis (FEA). A net cage with solidity of 0.23 was evaluated for current velocities from 0.1 to 0.5 m/s and compared with experimental data. The net cage was built up of three dimensional truss elements, which were given combined properties in order to represent parallel twines in the netting. Cross flow principle was assumed and forces was found using Morsion's equation for drag and lift. Velocity reduction was based on experimental data from [Løland, 1991]. The deformation was found by using iteration to find the relationship between the force and deformation. The method showed, in general, good comparison with measured data.

The use of computational fluid dynamics (CFD) to find the flow through and around net cages has also been performed.

[Patursson et al., 2006] investigated fluid through and around net panels with different angles of attack by modelling the net as a thin porous material. It was found that the method gave adequate results, but the porous media they used cannot be isentropic. This is because the flow resistance need to be larger inn the normal direction, compared with the tangential.

The use of porous jump material boundary was also performed by [Shim et al., 2009], with porosities varying from 0 to 90%. The method was chosen since modelling of every cylinder is both time consuming and computationally expensive. The results were compared with previous published experimental values for 5000 and 20000 Reynolds number. Reasonable estimation of drag coefficient and velocity profile was obtained.

In 2011 a full scale testing with Permaskirt was launched. The results are presented in the report [Næs et al., 2012]. Nordlaks Oppdrett AS initiated the project in order to develop preventive methods to reduce the number of lice.

In contrast to the skirts used in this thesis, the skirt used in the experiment had a mesh size of  $350\mu m$ . This mesh size was chosen to reduce the forces on the structure and ensure satisfying oxygen level in the net cage. The copepodites, which are the salmon lice infective larval stage, have a width of  $250\mu m$ , and may have gotten through the skirt. Investigations regarding lice passing through the skirt was not performed and is

mentioned as an error source.

The project lasted for seven months and the number of lice were counted once every week. For the net cages without a skirt, the average number of lice per fish varied between 0.17 and 0.23. In contrast, the net cages with a skirt attached had an average of 0.05 to 0.07 lice per fish giving it a reduction factor of approximately 4.

As this project had a biological scope, forces and deformation on the skirt was not measured. However, some problems with skirt deformation occurred when the skirt was lifted above the free surface. The reduction of lice, obtained in this full scale experiment, will be used as comparison when estimating the effect of Permaskirt with CFD calculation.

## 1.5 Previous calculation methods

To calculate the current forces and deformation on a net cage, there has been developed different methods. They differ in both complexity and precision. In this chapter, some of these will be explained in order to see the differences.

### 1.5.1 Projected area method

This method is presented in [Løland et al., 1988] and is one of the simplest methods to calculate the drag force on a net cage. The entire net cage is assumed as a rigid, solid cylinder without any water flow through the walls. As a consequence, there will not be any deformation and the drag force can be calculated as on a regular cylinder in current. The drag force can then be written as:

$$F_c = \frac{1}{2} * \rho * Cd_{cyl} * A_p * U^2 \quad (1.1)$$

$$A_p = D * h \quad (1.2)$$

Where  $A_p$  (eq. 1.2) is the projected area of the large cylinder, normal to the current direction calculated by multiplying the diameter  $D$  with the depth of the net cage cylinder,  $h$ .  $Cd_{cyl}$  is the drag coefficient and  $U$  is the current velocity.  $Cd_{cyl}$  is set as 1.0 or 1.5 depending on the distance between the net cages in the fish farm as a function of diameter of the individual net cage. This is a very simplified method and is intended for an approximate estimate in the early stages a project.

## 1.5.2 Potential flow theory

In order to find the pressure distribution around a circular cylinder, potential flow theory may be applied. The use of potential flow requires some assumptions. For this problem the incompressible ambient flow was assumed to be steady, uniform and the velocity potential satisfied the Laplace equation.

For a Permaskirt with single weights attached to it, the skirt pattern will look like figure 1.3, with several stagnation points. The number of stagnation points will vary with the number of weights. This effect was neglected for the potential flow calculation, and a circular cylinder without deformation was assumed.

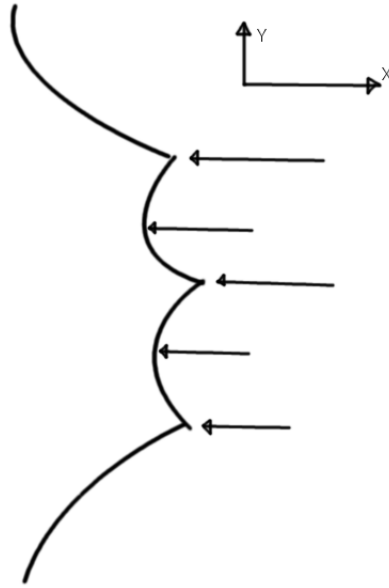


Figure 1.3: Markings of some of the stagnation points on a skirt in a two dimensional plane, seen from above. In this figure, the current travels in the negative x-direction.

Based on this, the pressure distribution may be found from Bernoulli's equation, given as

$$p + \rho \frac{d\phi}{dt} + \frac{\rho}{2} |\nabla\phi|^2 + \rho g z = Constant \quad (1.3)$$

where  $\phi$  is the velocity potential,  $p$  is the pressure,  $\rho$  is the density of water,  $g$  is the acceleration of gravity and  $z$  is the distance from the free surface to the point of evaluation.

Equation 1.3 can then be written as

$$p + \frac{1}{2}\rho U_t^2 = p_0 + \frac{1}{2}\rho U^2 \quad (1.4)$$

where  $p_0$  is the ambient pressure and  $U_t$  is the tangential velocity defined as

$$U_t = 2U \sin\theta \quad (1.5)$$

around a cylinder. Here,  $\theta$  is the angle between the incident flow,  $U$ , and  $U_t$ . For  $\theta = 0$  stagnation pressure is found.

Equation 1.4 can then be written as:

$$p = p_0 + \frac{1}{2}\rho U^2 - \frac{1}{2}\rho U_t^2 \quad (1.6)$$

which is used to find the pressure on the cylinder for a given angle and depth.

### 1.5.3 Forces on a three dimensional net cage

[Fredheim, 2005] developed a model to calculate the forces on a three dimensional net cage. In order to find the forces on a net cage with knotted mesh, the three dimensional net structures were divided into discrete elements. The twines between the knots were modelled as separate cylinders with two dimensional properties. Equation 1.7 was then used to find the drag force on each cylinder.

$$F_c = \frac{1}{2} * \rho * C d_{cyl} * d * L * |U| * U \quad (1.7)$$

Where  $U$  is the current velocity,  $C d_{cyl}$  is the drag coefficient for a twine cylinder,  $d$  is the diameter of the twine and  $L$  is the length of the twine between knots.

The knots were modelled as separate spheres with three dimensional properties. For these spheres, the drag force was found by

$$F_s = \frac{\pi * d^2}{8} * C d_{cyl} * |U| * U \quad (1.8)$$

Here,  $\frac{\pi * d^2}{8}$  is the projected area of the sphere.

The total force was then found by summation of the forces for each element. Interaction effect caused by the proximity of each element was not included, and this simplified method is therefore independent of the solidity.

## 1.6 FhSim simulation

In this thesis, the results have been compared with both measured data from experiment and calculated results by the simulation tool FhSim [Rundtop and Lien, 2013].

The report describes the use of FhSim to calculate the forces and deformation on a net cage fitted with Permaskirt. FhSim is developed by SINTEF for simulation and visualization of operations and systems.

FhSim uses numerical models of different components in order to do time domain simulations. As a result, forces and displacements can be found. The components may be placed together and exchange data using input and output ports. FhSim can simulate complex models by the use of substructures. Substructures, like floater tube, net, sinker tube and ropes, are used to simulate a net cage.

In the simulation, uniform and time invariant current was used. Meaning that the current velocity was constant in both time and vertical position under the free surface. The floater tube is made flexible by default in order to obtain realistic movement in waves. However, as there were no waves, it was made rigid enough to reduce the risk of becoming oval. In FhSim, the net is created as the sum of triangular elements, where each element consists of three nodes. These nodes connect each element in order to create a mesh with desired geometry.

The report was chosen for comparison in order to see how different simulation tools calculate the drag force and deformation on a net cage fitted with Permaskirt.

## 1.7 Load formulation in AquaSim

When the Norwegian Standard, NS 9415, was released, new methods to calculate forces and deformation on net cages had to be developed. [Berstad et al., 2004] introduced the finite element simulation tool AquaSim. The idea behind the finite element method is to establish equilibrium between the external acting forces, and the internal reaction forces.

In order to find the forces on a net cage, the twine in wake method is used [Berstad et al., 2012]. The method takes base in the solidity of the net in order to find the forces. AquaSim uses two formulas for the solidity, one for knotless mesh (eq. 1.9), and one for a knotted mesh (eq. 1.10).

$$S_n = \frac{d}{Ly} + \frac{d}{Lz} - \frac{2 * d^2}{Ly^2 + Lz^2} \quad (1.9)$$

$$Sn_{kn} = \frac{d}{Ly} + \frac{d}{Lz} + \frac{k * d^2}{2(Ly^2 + Lz^2)} \quad (1.10)$$

$k$  is a constant, typically 1 or 2.  $d$  is the diameter of the twine, while  $Ly$  and  $Lz$  is the twine length between knots in y and z direction. There is also a simplified 2D formula given as

$$Sn_{2D} = \frac{d}{Ly} + \frac{d}{Lz} \quad (1.11)$$

When the solidity is found, the drag coefficient for the net, or membrane,  $Cd_{net}$ , is found as

$$Cd_{net} = Cd_{cyl} * \frac{1}{(1 - \frac{Sn}{2})^3} \quad (1.12)$$

$$Rn = \frac{U * d}{\nu} \quad (1.13)$$

Where  $Cd_{cyl}$  is the drag coefficient for a single twine. It is given as a function of Reynolds number, where Reynolds number is given in eq. 1.13. The diameter in the formula,  $d$ , is the diameter of a single twine. Typical twine diameter,  $d$ , is  $0.001m$  and design current velocity is typically  $1m/s$ .  $\nu$  is in order of magnitude  $10^{-6}$ , which gives a Reynolds number (eq. 1.13) in order of magnitude  $10^3$ . This will give a drag coefficient,  $Cd_{cyl}$ , of approximately 1 according to figure 1.4.

The forces on the net, taking into account inflow direction and using the cross flow principle, can then be found as

$$F_n = 0.5 * \rho * Cd_{net} * d * L * v_n^2 \quad (1.14)$$

$$F_t = 0.5 * \rho * \pi * Ct * d * L * v_t^2 \quad (1.15)$$

Where  $F_n$  is the load normal to the twine and  $F_t$  is the transverse load.  $Ct$  is typically around 1-2% of  $Cd_{net}$ .  $v$  is the inflow velocity relative to the twine and is found by

$$v = U + v_w - v_m \quad (1.16)$$

Where  $U$  is the current velocity,  $v_w$  is the fluid velocity induced by the wave motions and  $v_m$  is the velocity of the mesh.  $v_n$  and  $v_t$  is the normal and tangential velocity component of  $v$ .

However, there are some limitations with this method. The method does not account for the fact that nets with the same solidity may have different drag properties. It also does not account for the boundary layers of the flow. For the case with a Permaskirt,



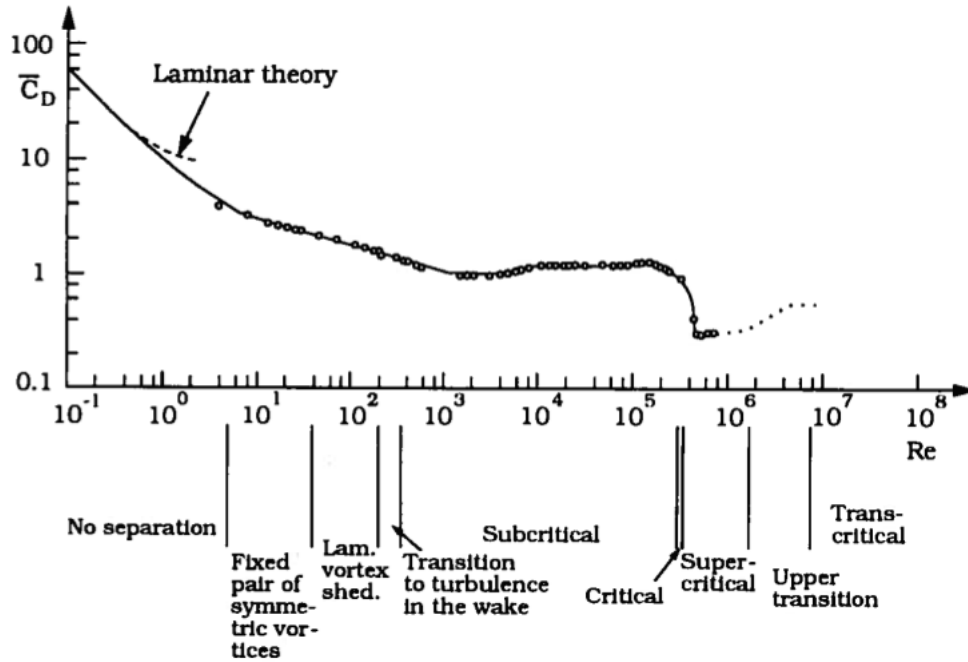


Figure 1.4: Drag coefficient,  $C_{d_{cyl}}$ , as a function of Reynolds number. Courtesy: [Sumer and Fredsøe, 2006].

AquaSim does not account for that the current may go around the net panel. These error sources are discussed in chapter 3.4.1.

### 1.7.1 Reduced velocity.

An option in AquaSim is the reduced velocity option, taking into account that water flowing through a net will experience reduction in velocity. How much the flow will decrease, depends on the solidity of the net. For the flow velocity reduction in AquaSim, the program uses the formula developed in [Løland, 1991]. The reduction factor  $r_r$  is defined as

$$r_r = \frac{u}{U} \quad (1.17)$$

where  $u$  is the velocity through the net and  $U$  is the free flow velocity. The velocity on the succeeding net, with distance large enough to neglect upstream effect will then be given as

$$U_1 = U * r_r \quad (1.18)$$

where  $U_1$  is the velocity on the first succeeding net.  $r_r$  can be found from the drag coefficient, using the following relationship:

$$r_r = 1.0 - 0.46Cd_{net} \quad (1.19)$$

Here,  $Cd_{net}$  is the drag force coefficient for the net in front of the net investigated. Løland showed by experiment how difficult it is to give a proper estimation for this drag coefficient based on the solidity for the net. If experimental values for the net evaluated are not possible to obtain, the following estimated functional relationship may be used:

$$Cd_{net} = 0.04 + (-0.04 + 0.33Sn + 6.54Sn^2 - 4.88Sn^3)Cos(\theta) \quad (1.20)$$

However, both equation 1.19 and 1.20 are simplified formulas developed for a solidity between 0.1 and 0.3. It is also assumed uniform wake in the transverse direction. This is not the case for the flow in the wake behind a net, with angle to the flow direction.

In order to see the effect of this formulation in AquaSim for higher solidity, two different trials were performed and are presented in chapter 3.2.1.

## 1.7.2 Finite element analysis

In order to calculate forces and displacements on a net cage, AquaSim utilize finite element analysis (FEA) [Berstad, 2013]. The method is based on Hooke's law which states that the force,  $F$ , needed to extend or compress a spring by a distance of  $\Delta l$  is proportional to that distance by a stiffness coefficient  $k$ :

$$F = k\Delta l \quad (1.21)$$

To obtain equilibrium, there must be equilibrium between external forces applied to the element and internal forces. Finite element analysis divides a structure into a finite number of elements, with a finite number of degrees of freedom, and finds equilibrium in each element and the whole structure.

During the calculation, the external force is incremented in order to find equilibrium for each step. For each step the external force is calculated based on displacement in the previous step, and a new displacement is predicted. These iterations are increased until convergence is established.

## 1.8 CFD analysis

To find pressure and flow distribution around a Permaskirt in current, Computational Fluid Dynamics (CFD) is a useful tool. CFD is a discipline within fluid mechanics which make use of numerical models and algorithms. The basis for most numerical software is the Navier-Stokes equations which describes the motion of viscous fluids [White, 2006].

For this thesis, the software Ansys Fluid with Reynolds-averaged Navier-Stokes approach has been used. Ansys software is a large collection of different programs integrated in the Ansys Workbench software. CFD calculations executed in the Ansys Fluent software can be used in order to model flow, turbulence, heat transfer, and reactions.

A simplified version of the Navier-Stokes equations, [Cebeci and Cousteix, 2005], can be written as

$$\frac{\partial U}{\partial x} + \frac{\partial V}{\partial y} + \frac{\partial W}{\partial z} = 0 \quad (1.22)$$

$$\rho(U \frac{\partial U}{\partial x} + V \frac{\partial U}{\partial y} + W \frac{\partial U}{\partial z}) = -\frac{\partial P}{\partial x} + \mu \frac{\partial^2 U}{\partial y^2} + \rho \frac{\partial}{\partial y}(-\overline{u'v'}) \quad (1.23)$$

$$\rho(U \frac{\partial W}{\partial x} + V \frac{\partial W}{\partial y} + W \frac{\partial W}{\partial z}) = -\frac{\partial P}{\partial z} + \mu \frac{\partial^2 W}{\partial y^2} + \rho \frac{\partial}{\partial y}(-\overline{v'w'}) \quad (1.24)$$

when the boundary layer thickness  $\delta$  is sufficiently small compared with the reference length. They are referred to as the boundary-layer equations. Here,  $\rho$  is the density of the fluid,  $\mu$  is the dynamic viscosity.  $U, V, W, P$  are the mean values for the velocities in x,y and z direction and pressure.  $u, v, w, p$  are the instantaneous values and  $u', v', w'$  are the fluctuating part.

The Reynolds-averaged Navier-Stokes (RANS) equations above show that there are more unknowns than equations. It is therefore necessary to use turbulence models in order to express the Reynolds shear stresses in known variables. For this thesis, the k- $\epsilon$  model was used.

The k- $\epsilon$  model is a RANS-based turbulence model. It is a two-equation model for CFD and the purpose is to predict an eddy viscosity from velocities and time-scales,  $T = k/\epsilon$  [Durbin and Petterson-Reif, 2011]. The  $k$  represents the turbulent kinetic energy, and  $\epsilon$  represents the rate of turbulent dissipation. In turbulent flow, the molecular viscosity is of smaller importance. Therefore, an eddy viscosity representing transport and dissipation of energy at smaller scale is used.

The turbulent model is widely used within CFD analysis due to good convergence rate and low memory requirement.

# Chapter 2

## Modelling methods

### 2.1 Potential flow theory

Pressure distribution calculated by potential flow theory was investigated and compared with AquaSim and CFD results to see if there were any similarities in the distribution. The numerical computation tool Matlab was used for potential flow calculation.

In order to achieve comparable data, the input in Matlab was the same as in AquaSim. In z-direction, the height was set as  $0.363m$  and divided into 20 elements. In x-direction, the distance was set as  $\pi$ , from  $-\frac{\pi}{2}$  to  $\frac{\pi}{2}$  and divided into 54 elements such that the mesh became equal to the one modelled in AquaSim. The angle  $\theta$  [deg] is from now on used to explain the angle between the net and the incoming current.  $\theta = 0$  is the stagnation point. A loop function, using eq. 1.6, was then used to find the pressure for each node. Static pressure was neglected since only dynamic pressure is of interest. The results were then plotted as a graph with colors representing the force.

### 2.2 Model testing of a net cage with Permaskirt

The main part of this thesis is based on an experiment executed by SINTEF in Hirtshals [Lien and Volent, 2012], which was performed in order to find deformation and forces on a net cage fitted with Permaskirt.

The experiment was a part of the project "Permanent skjørt for redusering av luspåslag på laks" (Permanent skirts for reduction of lice spread on salmon) financed by Fiskeri- og havbruksnæringens forskningsfond (FHF) and Norwegian industrial partners. The purpose of the experiment was to investigate the forces acting and the following deformation on a net cage with a skirt attached to it. As a result, the measured data will contribute in setting limitations for the use of Permaskirt in different environmental conditions and

give knowledge about forces on a net cage fitted with Permaskirt.

A net cage, 157 meters in circumference, was scaled 1:17 ( $\lambda = 17$ ) and tested with different skirt configurations and current velocities. The net cage used as basis for the configuration, had a cylindrical net with flat bottom.

The test model was made as a conventional net cage with two 32 mm SDR 11 PE80 floating tubes held together with 16 brackets. The net, with a solidity of 0.21 was attached to the inner floating tube and weighted down by a sinker tube. The sinker tube was made of the same material as the floating tubes, but perforated and had a brass chain inside it to increase the weight. On the outer floating tube, the skirt was attached and had ropes connecting it with the sinker tube combined with 36 individual weights at the bottom of the skirt.

Forces on the mooring line, skirt, net deformation, and current velocity inside and outside of the net cage was measured. In this thesis, all of the measured values will be used as comparison for calculated data.

## 2.3 The AquaSim software package.

For this thesis, the software package AquaSim, developed by Aquastructures, has been used. The package consists of 5 individual programs, which are used to obtain the final results by utilizing finite element analysis (FEA).

When an analysis is to be initiated, the drawing program AquaEdit is opened. AquaEdit uses a graphical interface to draw a geometrical structure. Geometrical values, such as lengths and number of elements are given as input to give the model correct shape and size.

What kind of component each element is made of is also selected. Beam, truss, or membrane may be chosen in order to create a full net cage. For this thesis, typical component selection was beam for the tubes, truss for the mooring line and membrane for the skirt and net cage. After the geometrical model has been made and saved, the drawing part is finished and AquaEdit is closed.

The next step, is then to open AquaBase. Here, all the structural and hydrodynamic properties are established. All values regarding stiffness, weights and geometrical inputs for the elements are inserted manually. The external forces, such as waves and current are provided by the user and exported as a .bat file, which is used by the AquaSim solver.

The solver uses finite element analysis, described in chapter 1.7.2 and is the program that derives the results from the given input of geometry, structural properties and en-

vironmental properties provided by AquaEdit and AquaBase. The solver accounts for hydro elasticity, so deformations and changes in the structure will lead to changes in the loads acting on the structure. As the results are obtained, they are exported into .AVS- and .AVZ-files which are used for post processing.

Post processing are done by using two different programs. AquaView presents the results graphically, with color a bar to display magnitude of forces, displacement etc.

In order to extract precise results for a given node or element, the program AquaTool is used. Results are given as a table and may be copied to a spreadsheet, such as Excel, for further post processing.

### 2.3.1 AquaSim modelling

To see how AquaSim calculate the forces with Permaskirt, the experiment by SINTEF in Hirtshals [Lien and Volent, 2012] and the SINTEF report [Rundtop and Lien, 2013], was used for comparison. The experiment in Hirtshals took base in a 49.9 meters in diameter fish cage, which was scaled 1:17. The tested model had therefore a diameter of 2.938m.

In order to see how AquaSim simulated the forces and deformations compared to the experiment, the model in AquaSim was made as accurate as possible. Figure 2.1 shows the key dimensions for the net cage used in the experiment. How the model was made in Hirtshals is explained in chapter 2.2.

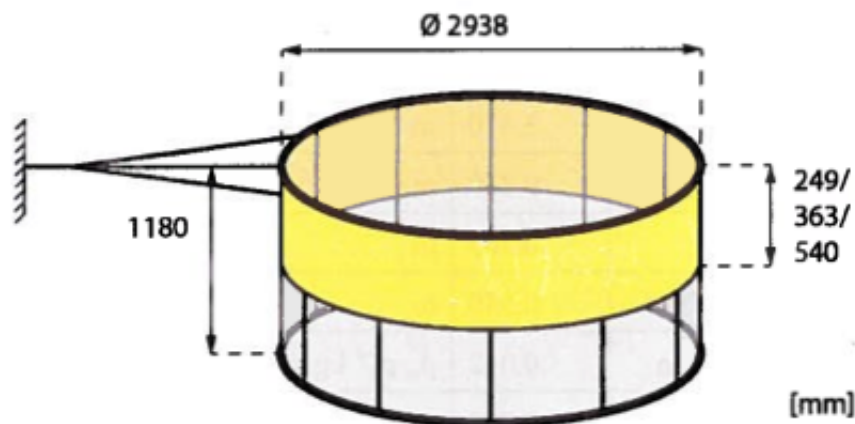


Figure 2.1: Key dimensions for the net cage. A skirt depth of 363mm was used for this thesis. Courtesy: [Lien and Volent, 2012].

To make the model in AquaSim, the first step was to open AquaEdit. Two circles were drawn at  $z = 0$  and set as beam to become inner and outer floating tube. Diameter for the inner floating tube was set to  $2.938m$  and outer floating tube had a diameter of  $3.119m$ . Each tube was divided into a total of 108 elements with 54 brackets holding them together. In the experiment only 16 brackets were used, but since the stiffness of the tubes and brackets was so high in the experiment, it could be regarded as a rigid element. The increase in brackets would therefore not cause any large differences in the results.

The net was extruded from the inner floating tube, down to a depth of  $1.18m$  with 45 steps, creating a mesh for the net.

At the bottom of the net, a sinker tube was modelled with the same dimensions as the inner floater tube.

A new mesh was then extruded from the outer floating tube, down to a depth of  $0.363m$  to become the skirt. Ropes was attached between the bottom of the skirt and the sinker tube, and nodes were selected to become the 36 individual weights at the bottom of the skirt.

At the fore part of the outer floating collar, a truss was attached as a mooring line. The end node at the truss, towards the incoming current, was locked in all translation directions to act as a mooring point. The complete fish cage, as modelled in AquaEdit is presented in figure 2.2.

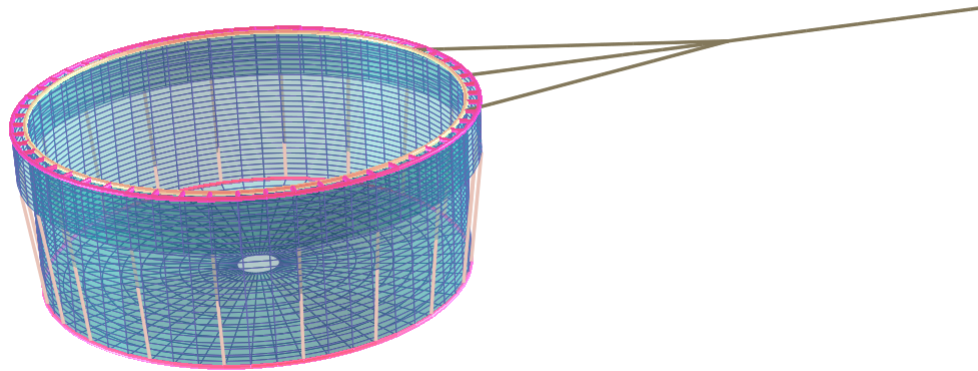


Figure 2.2: The fish cage as modeled in AquaEdit.

Full scale geometrical values for the net cage are presented in table 2.1, multiplication factors used for scaling are found in table 2.2 and the scaled geometrical values for the model net cage, as used in the experiment and AquaSim, are found in table 2.3.

Diameter inner floater tube	49.946	m
Diameter outer floater tube	53.023	m
Diameter sinker tube	49.946	m
Net depth	20.06	m
Skirt depth	6.171	m

Table 2.1: Full scale dimensions of the investigated net cage.

Size	Unit	Multiplication factor
Length	$m$	$\lambda$
Area	$m^2$	$\lambda^2$
Volume	$m^3$	$\lambda^3$
Force	$\frac{kg*m}{s^2}$	$\lambda^3$
Mass density	$\frac{kg}{m^3}$	1
Speed	$\frac{m}{s}$	$\sqrt{\lambda}$

Table 2.2: Multiplication factors used for scaling to model size.  $\lambda = 17$ .

Diameter inner floater tube	2.938	m
Diameter outer floater tube	3.119	m
Diameter sinker tube	2.938	m
Net depth	1.18	m
Skirt depth	0.363	m

Table 2.3: Scaled net cage dimensions used in the experiment and AquaSim simulations.

In order to give properties to the geometry drawn in AquaEdit, the file was saved and then opened in AquaBase.

For the tubes, a 500 mm tube was used as reference. This was found in the AquaBase library file. As the diameter of the tube in the experiment was 32 mm, the scaling factor,  $\lambda_2$ , was set to 15.625. This gave the floating tube correct geometrical values



compared with the experiment, but the stiffness was higher. Since the floating tubes in the experiment was rigid enough to avoid any deformations, an increase in the stiffness would have minimum effects for the simulated results.

Since the sinker tube was perforated and filled with water, the density became  $940 \frac{kg}{m^3}$  and therefore neglected. Thus, only the weight of the brass chain inside the sinker tube,  $1.422 \frac{N}{m}$ , was taken into account. Properties for the floating tubes and sinker tube are found in table 2.4 and 2.5.

Floating tubes	Value	Unit
E-modulus	$9E8$	$\frac{N}{m^2}$
G (Shear)	$3.462E8$	$\frac{N}{m^2}$
Area	$8.042E - 4$	$m^2$
I[z]	0.003	$m^2$
I[y]	0.02	$m^2$
I[t]	0.0039	$m^4$
Weight	2.68	$\frac{N}{m}$
Mass density	340	$\frac{kg}{m^3}$
Volume	0.0016	$\frac{m^3}{m}$

Table 2.4: Properties for the floating tubes in AquaSim.

Sinker tube	Value	Unit
E-modulus	$9E8$	$\frac{N}{m^2}$
G (Shear)	$3.462E8$	$\frac{N}{m^2}$
Area	$8.042E - 4$	$m^2$
I[z]	$2.7E - 4$	$m^2$
I[y]	$2.5E - 4$	$m^2$
I[t]	$5.4E - 4$	$m^4$
Weight	13.99	$\frac{N}{m}$

Table 2.5: Properties for the sinker tube in AquaSim.

The floater tubes were stiffer than what was the case in full scale. Regarding the forces and net deformation, this will have small influence. [Rundtop and Lien, 2013].

The net cage was split into two different parts, where the upper part was from the free surface and down to the skirt depth of  $0.363m$ . This was done due to the assumption that

Net	Value	Unit
E-modulus	$1E9$	$\frac{N}{m^2}$
Area	$3.14E - 6$	$m^2$
Pretension y	$5E - 5$	$N$
Pretension z	$5E - 5$	$N$
Mask width y	0.018	$m$
Mask width z	0.018	$m$
Mass density	1025	$\frac{kg}{m^3}$

Table 2.6: Properties for the net in AquaSim.

there will not be any water flowing through the skirt. If, however, water did flow through in the calculations, it would not increase the forces on the part of the net placed directly behind the skirt. For this part of the net, the solidity was set to 0.01.

The lower part of the net, directly influenced by the current, had a solidity of 0.21. Properties for the net, under the skirt, are found in table 2.6.

The skirt had the same E-modulus, pretension and density as the net. Twine diameter was set to  $0.001m$ , giving it an area of  $7.85 \cdot 10^{-7} m^2$ . Mask width in y- and z-direction were set equal to each other, making the mesh quadratic. The mask width was varied between 0.0034 and  $0.001m$  to vary the solidity between 0.5 and 1, calculated with equation 1.9. Twine diameter was constant throughout the calculations.

Information about what kind of mooring line used in the experiment was not mentioned in the SINTEF report. It was therefore set as  $1.5mm$  dyneema line to minimize effects from current on the mooring line. The same properties were used for the lines connecting the skirt to the sinker tube. Properties are found in table 2.7.

Mooring line	Value	Unit
E-modulus	$8E9$	$\frac{N}{m^2}$
Area	$1.76E - 6$	$m^2$
Mass density	1025	$\frac{kg}{m^3}$

Table 2.7: Properties for the mooring line in AquaSim.

## 2.4 Ansys CFD

In order to find pressure and flow distribution around a Permaskirt in current, CFD analysis was performed. To perform these calculations, the Ansys software package was used.

The Ansys software package is a large collection of different programs integrated in the Ansys Workbench software. CFD calculations are executed in the Ansys Fluent software and can be used in order to model flow, turbulence, heat transfer, and reactions.

The CFD calculations took base in the model size of the skirt, which was used in both the experiment and AquaSim calculations. For a more realistic simulation regarding the effects of a skirt around a net cage, a full scale model with net cage included should have been used. However, due to little information about this kind of simulation, only the skirt in model scale was used. The advantages with this kind of simulation, was the possibility to compare CFD results with experimental data. It was therefore possible to evaluate the use of CFD to simulate the flow distribution around a deformed skirt.

### 2.4.1 Ansys modelling

For the CFD calculations, there were made two different models. The first model (M1) was made as a cylinder without any deformation, while the other (M2) had deformation. A model without any deformation was necessary since the calculations with both potential flow theory and pressure in AquaSim was without any deformation. In order to see the effect of Permaskirt with respect to current and flow distribution, a deformed skirt had to be applied. Both models consisted of the skirt only, i.e. net cage, chains and tubes were neglected.

The first model (M1) had the same inputs as those used in AquaSim, with a diameter of  $3.119m$  and a depth of  $0.363m$ . For the second model (M2), the deformation pattern was extracted from AquaSim for the case with skirt only and a solidity of 0.6. The case in AquaSim was selected since it was the one that gave best comparison with measured data, and accurate three dimensional coordinates for the deformed shape could be extracted. Some simplifications had to be done with the deformation pattern for M2 since the program was not able to create the surface. The deformation pattern, shown in figure 1.3, had to be neglected. The deformed and simplified Ansys model (M2) is shown in figure 2.3.



Figure 2.3: Model M2 as modelled in Ansys, seen from the left. The deformation had to be simplified due to complex geometry.

In order to test under the same conditions as in Hirtshals, the fluid domain was given the same size as the flume tank with 21.3 meters in length, 8 meters in width and 2.7 meters in depth. The skirt was placed in the center of the fluid domain with the top of the skirt at the free surface.

Different mesh sizes, with number of elements varying from  $0.9 \times 10^6$  to  $5.6 \times 10^6$  was simulated. The case in this report had a total of  $2.9 \times 10^6$  elements. Figure 2.4 shows the mesh used in the simulation.

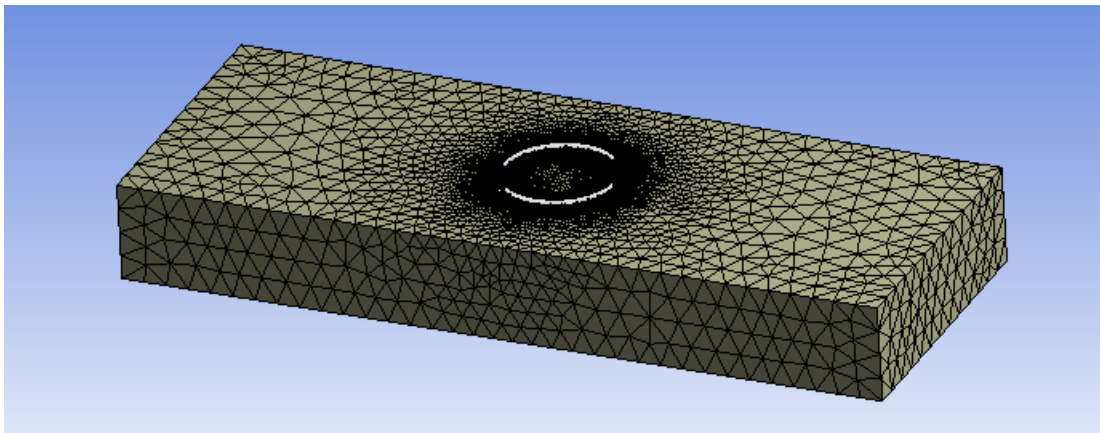


Figure 2.4: Meshing for the fluid domain in the simulation.

The choice of mesh presented in this thesis was based on a mesh refined study. A point placed in the center of the skirt and  $0.2m$  below the free surface was used for velocity

measurements. The velocity at this point, for each mesh, was then plotted and compared to see if it converged. As seen from figure 2.5, the velocity converges against  $0,04466m/s$ . The model with  $2.9 \times 10^6$  elements was chosen since it gave accurate velocity measurements ( $0.0446594m/s$ ) and higher mesh refinements would cause the computer to run very slow.

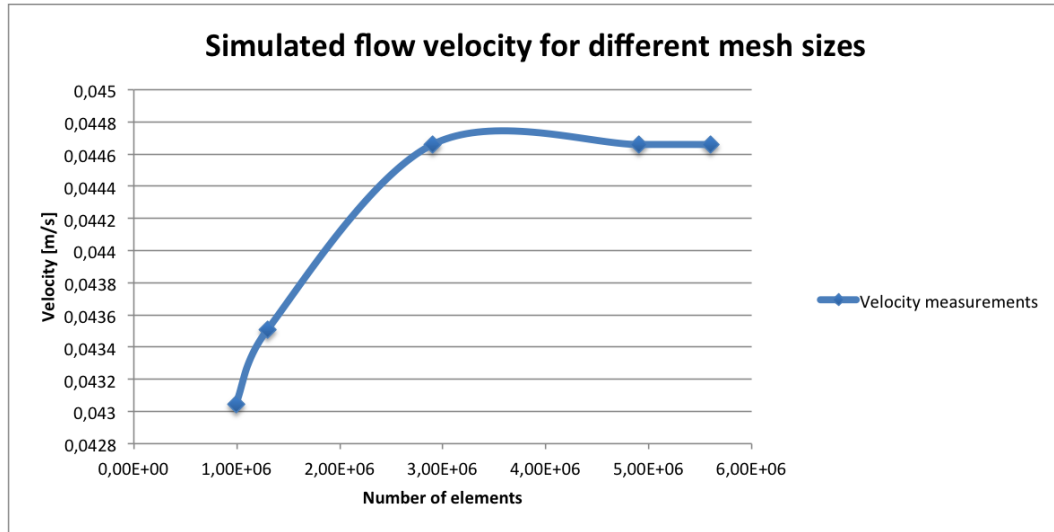


Figure 2.5: Velocity measurements for different mesh sizes used for checking mesh refinement.

A pressure based steady state Reynolds-averaged simulation (RAS) with realizable  $k-\epsilon$  turbulence model and non-equilibrium wall functions was used for the simulation.

A steady state simulation gives an average of the flow distribution. Current velocity was set to  $0.1 m/s$  giving it a Reynolds number, with respect to the diameter of the skirt, of  $3.1 \times 10^5$ . This indicate a critical flow regime [Sumer and Fredsøe, 2006] which may cause an unstable wake at the aft part of the skirt which is not detected by steady state simulation.

The fluid was set as fresh water with a density of  $988.2 \frac{kg}{m^3}$  and a dynamic viscosity of  $0.001003 \frac{kg}{m \cdot s}$ . The two sidewalls and the bottom of the tank was given no-slip wall conditions. This gives zero particle velocity at the walls and prevents the water to flow through the sidewalls and bottom. For the free surface, slip condition was given in order to prevent friction between water and air. The skirt surface was given the same conditions as for the walls and bottom of the tank. At the inlet, the current velocity was set to  $0.1m/s$  and was uniform over the cross section.

The calculations were initiated with 100 iterations, where a coupled pressure-velocity scheme with first order upwind spatial discretization for momentum, turbulent kinetic energy and turbulent dissipation rate were used. After these initial iterations, first order upwind was changed to second order upwind and the iterations were continued until convergence was achieved.

# Chapter 3

## Results and discussion

### 3.1 Pressure distribution

In order to investigate the dynamic pressure distribution on a Permaskirt, different methods to calculate the pressure on the skirt was performed with  $0.2m/s$  current velocity. Potential flow theory, CFD and AquaSim was used in order to find the pressure.

Only the pressure on the front part of the skirt was investigated. The Reynolds number for the case,  $3.1 * 10^5$ , indicates critical flow regime (fig. 1.4), which would not be detected by the different methods, giving large error values especially at the aft position of the skirt.

Results from potential flow theory are shown in figure 3.1. Maximum value, at stagnation point, is 20.24 Pa and minimum value, at  $\theta = 90deg$  is -61.45 Pa.

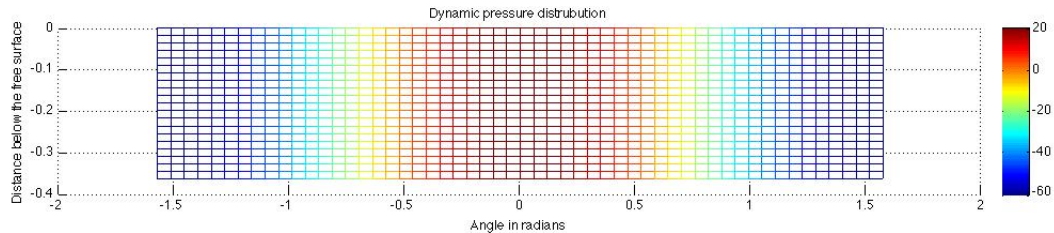


Figure 3.1: Dynamic pressure distribution on the net, calculated by potential flow theory in Matlab.

Figure 3.2 shows the different pressure distributions from 0 to 90 degrees for all three methods. As seen from the figure, the dynamic pressure at the stagnation point is lower in AquaSim compared to the potential flow and CFD calculations. The pressure calculated

by AquaSim was found by extracting the forces in X- and Y-direction and dividing it on the projected area for each element.

At the stagnation point, the pressure was found to be about half of what was calculated by the other two methods. Maximum value, for  $\theta = 0deg$ , is  $12.25Pa$  and minimum value, at  $\theta = 90deg$ , is  $\approx 0$ . As the angle approached 90 degrees, the pressure approached 0. This was expected since AquaSim is a finite element program and does not account for velocity distribution around the construction.

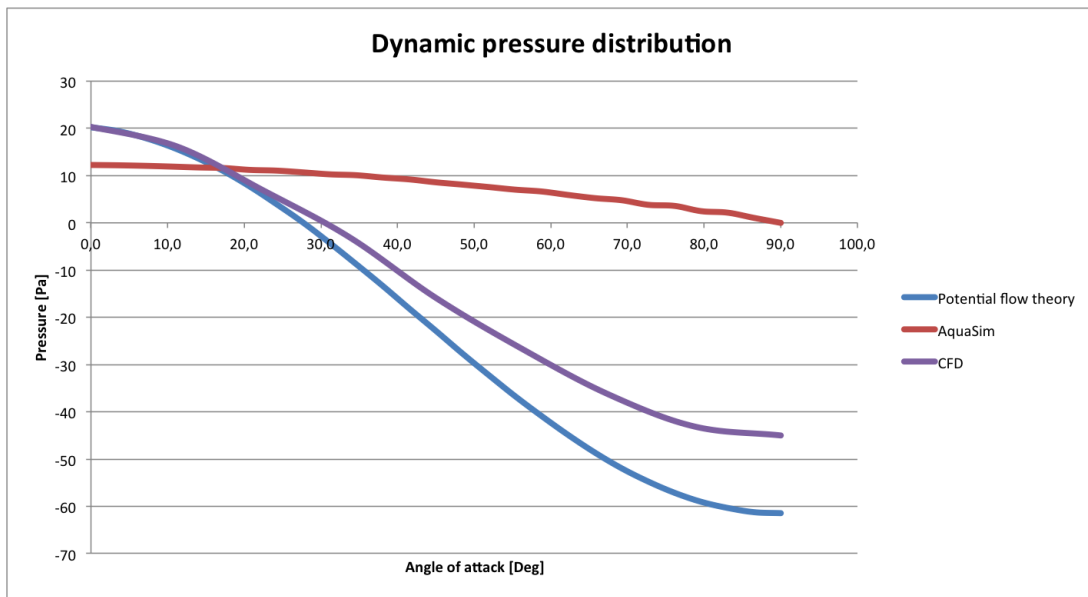


Figure 3.2: Dynamic pressure distribution calculated by potential flow theory, CFD and AquaSim.

The CFD values are almost identical with potential flow theory from 0 to 20 degrees. However, the lowest pressure in the CFD calculation is -45 Pa and there is some deviation. The results from potential flow theory and CFD are as expected [Faltinsen, 1990].

## 3.2 AquaSim results

The AquaSim model used for the calculations has been explained previously. For the modelling process, the main focus has been to make the model as accurate as possible with regard to the model in the experiment.

The drag force was found by extracting the axial force from an element in the mooring truss, which was the same method used in the experiment [Lien and Volent, 2012]. For



the deformation results, the average depth for three nodes fore and aft at the bottom of the skirt was used and is presented as percent of initial depth [Rundtop and Lien, 2013]. The results are presented as plots, while tabulated data are found in appendix A.

### 3.2.1 Reduced velocity

The reduced velocity option in AquaSim is described in chapter 1.8.1. In order to see the effect of this formulation in AquaSim, two different test trials were performed with the skirt only configuration and a solidity of 1. Since the solidity is outside the range of which the formulation (eq. 1.19) is developed and there should not be any water flowing through the skirt, it is of interest to see how this option affects the results.

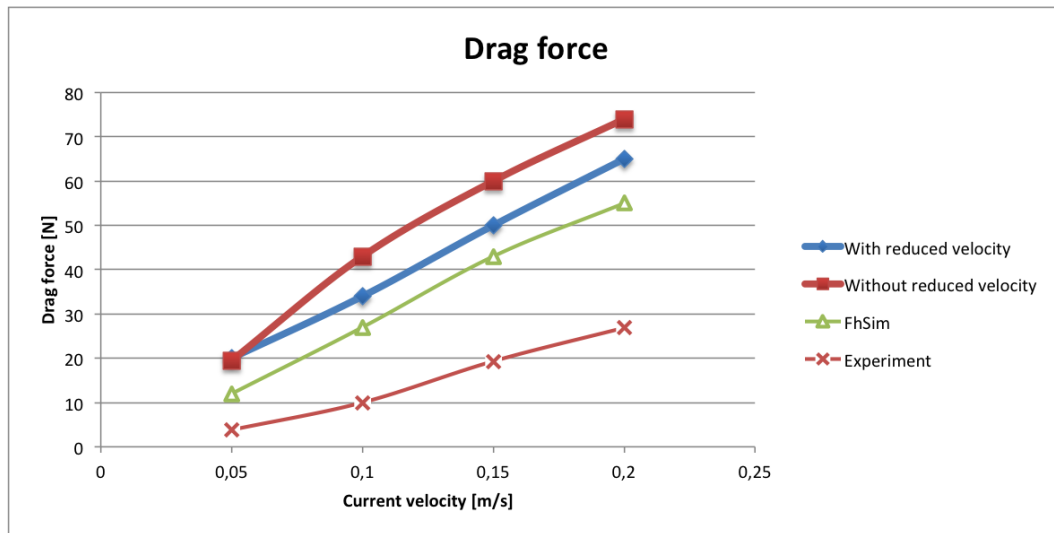


Figure 3.3: Drag force, with and without reduced velocity enabled in AquaSim. All results from skirt only configuration.

As expected, the drag force is reduced when current reduction on succeeding nets are enabled (fig. 3.3). At the initial velocity of  $0.05\text{m/s}$  there is a small difference of only 2% between the two methods in AquaSim, while it is between 16 and 20% for the other velocities. Results from FhSim and experiment are also included in the plot, and both test trials from AquaSim overestimates the values compared with the other two methods.

Using eq. 1.20 and evaluating the foremost panel where  $\theta = 0$ ,  $S_n = 1$  gives a drag coefficient ( $C_{d_{net}}$ ) of 1.99. The reduction factor,  $r_r$ , will then become 0.0846 (eq. 1.19). Since the velocity on the first succeeding net, eq. 1.18, is given as the free flow velocity times the reduction factor,  $r_r$  should become zero for  $S_n = 1$ . However, as shown in

figure 3.3, current reduction should be enabled and it is therefore enabled for all trials performed in this thesis.

### 3.2.2 Full configuration

The full configuration consisted of the net cage and skirt as it would be mounted in operating condition.

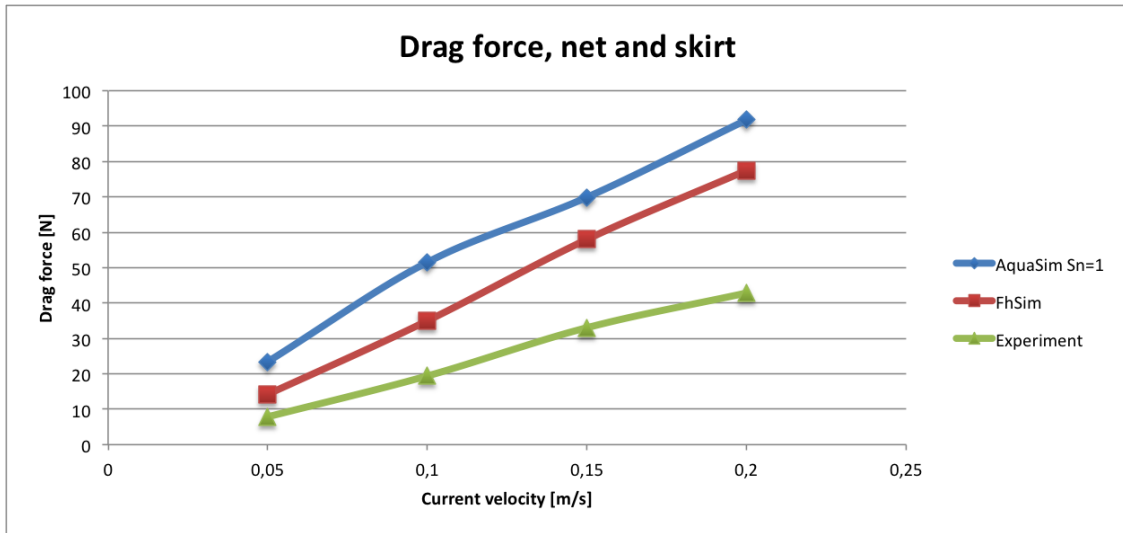


Figure 3.4: Drag force on the net cage, fitted with Permaskirt. Comparison between AquaSim, FhSim and experimental values. All for  $S_n=1$ , which implies a watertight skirt.

Figure 3.4 shows the drag force on the net cage. The forces were extracted as axial force in an element in the mooring line. The deviation, with respect to experimental values, is 197% for  $0.05\text{m/s}$  and is reduced to 114% at  $0.2\text{m/s}$ . There is also overestimation compared with calculated results in FhSim.

Comparing results for the net cage without Permaskirt (table A.4) with results for full configuration, the drag force increased 86, 61, 51 and 36% for the four current velocities investigated when a skirt is fitted to the net cage. The effect of mounting a skirt around a net cage will therefore give largest percentage increase in drag force for the lowest current velocities.

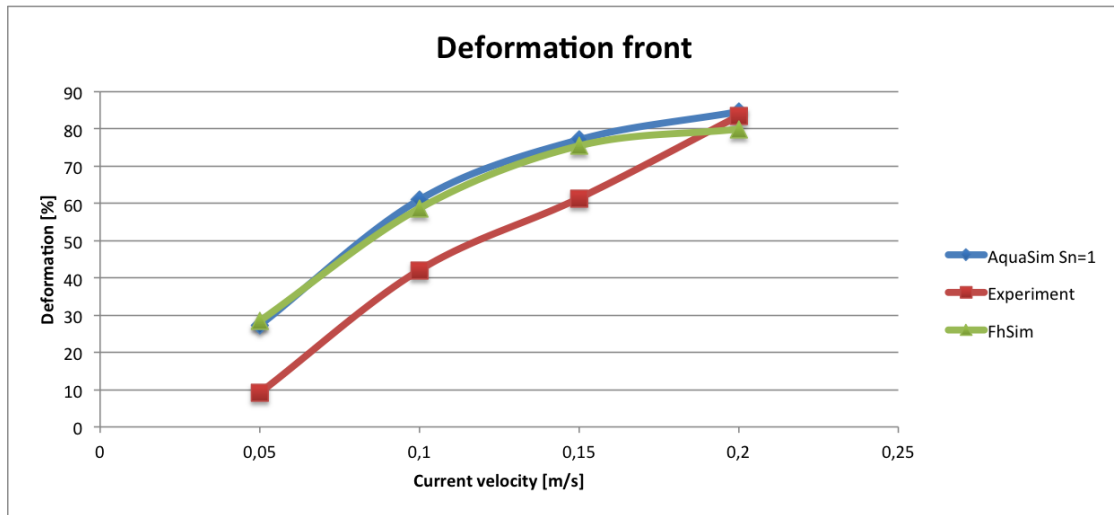


Figure 3.5: Deformation on the fore part of the skirt, for the case with both net cage and Permaskirt. Comparison between AquaSim, FhSim and experimental values. All for  $S_n=1$ , which implies a watertight skirt.

Skirt deformation on the front part of the skirt (fig. 3.5) shows good resemblance with the calculations in FhSim. There is large overestimation at lower current velocities, which is reduced as the current velocity increased.

For  $0.2\text{m/s}$  there was only a small difference in the calculated values compared with the measured one.

A reason for the overestimation is that AquaSim does not take into account friction between the skirt and net cage when the skirt is pushed into the net cage. It was therefore only the ropes, connecting the skirt with the sinker tube, which prevented deformation.

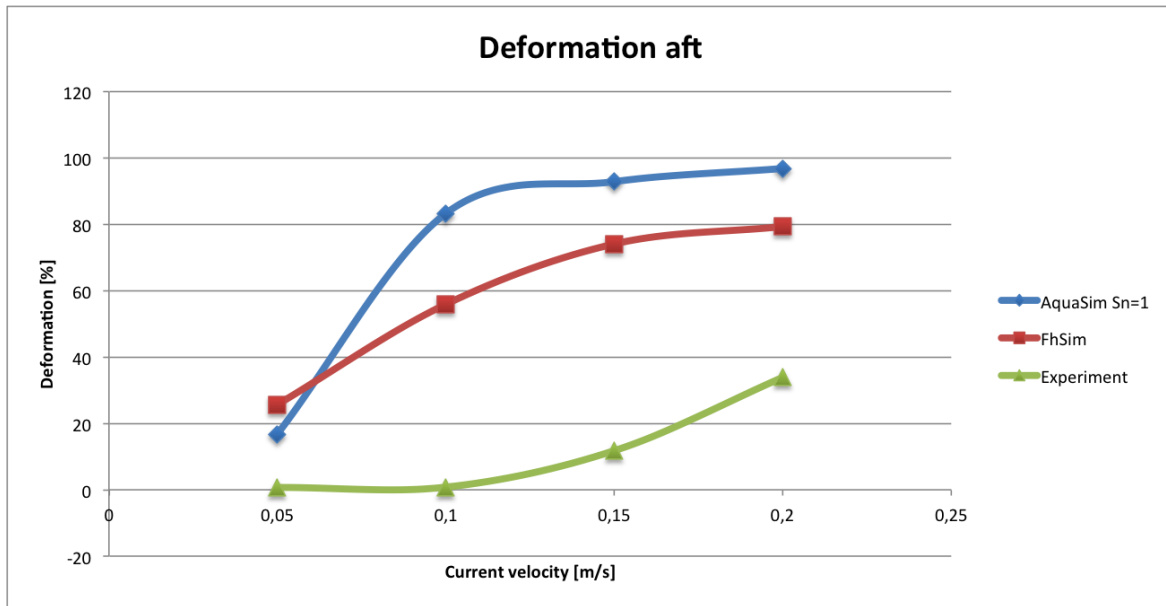


Figure 3.6: Deformation on the aft part of the skirt, for the case with both net cage and Permaskirt. Comparison between AquaSim, FhSim and experimental values. All for  $Sn=1$ , which implies a watertight skirt.

The skirt deformation aft (fig. 3.6) shows larger deviation than the ones on the fore side. When the current velocity is increased from  $0.05$  to  $0.1\text{m/s}$  a large increase in deformation is observed in the AquaSim simulation. For further increase in current velocity, the curve flattens out. Compared with experimental values, it is observed that the deformation pattern obtained in AquaSim gives a large error and this kind of calculation should be used with care.

The large deformation at the aft position of the skirt may be a result of higher current velocity at this part, compared with experimental values.

In order see the effects of skirt solidity, regarding drag force and deformations, different trials were executed. Figure 3.7 shows the drag force when the solidity was varied between  $0.9$  and  $0.6$ . Values obtained in FhSim and experiment, for  $Sn = 1$ , have also been included for comparison. It is observed that reducing the solidity from  $1$  (fig. 3.4) to  $0.9$  gives a large reduction in the drag force. As the solidity is further reduced, the reduction in drag force for each calculation is decreased. A solidity of  $0.6$  gives very accurate values for the lower velocities, while  $Sn = 0.7$  represent the higher velocities in a more accurate manner compared with experimental values.

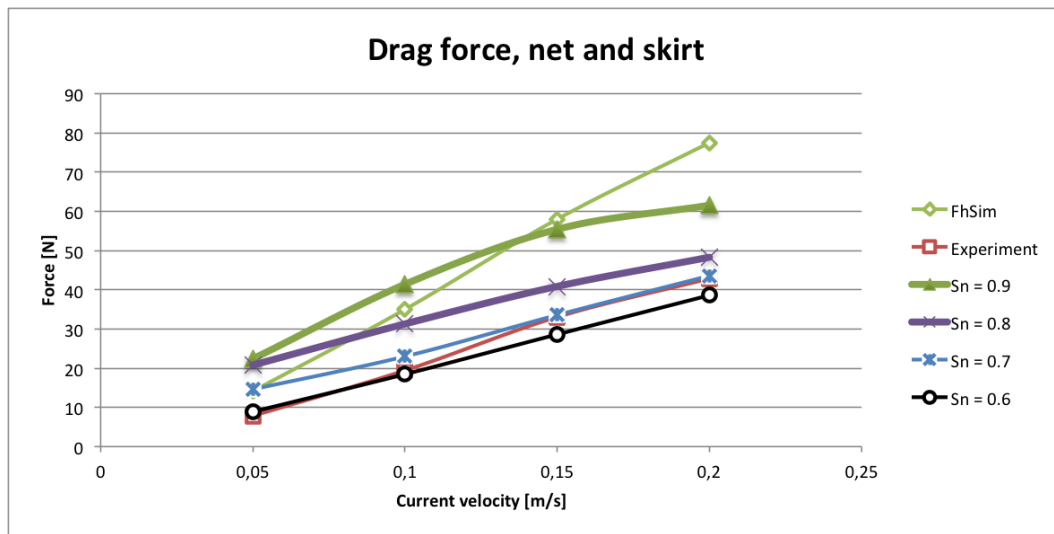


Figure 3.7: Drag force on the net cage, fitted with Permaskirt.  $Sn = 0.9$  to  $0.6$  indicates the varying solidity in AquaSim. Both FhSim calculation and experimental test values was obtained with  $Sn=1$ .

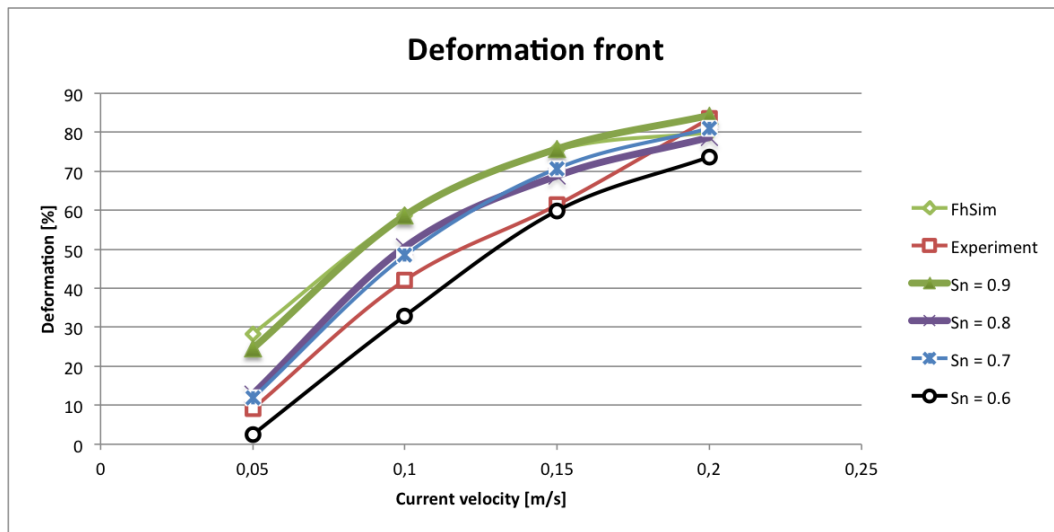


Figure 3.8: Deformation on the fore part of the skirt attached to the net cage.  $Sn = 0.9$  to  $0.6$  indicates the varying solidity in AquaSim. Both FhSim calculation and experimental test values was obtained with  $Sn=1$ .

Figure 3.8 shows the deformation at the fore part of the skirt as percent of initial skirt depth. For a solidity of 0.9, the results are quite accurate compared with FhSim calculations. Reducing the solidity to 0.8 gives smaller deformation, while a solidity reduction from 0.8 to 0.7 gives very small changes in deformation.  $Sn = 0.8$  and 0.7 underestimates the deformation for  $U = 0.2m/s$ , while a solidity of 0.6 underestimates the deformation for all current velocities.

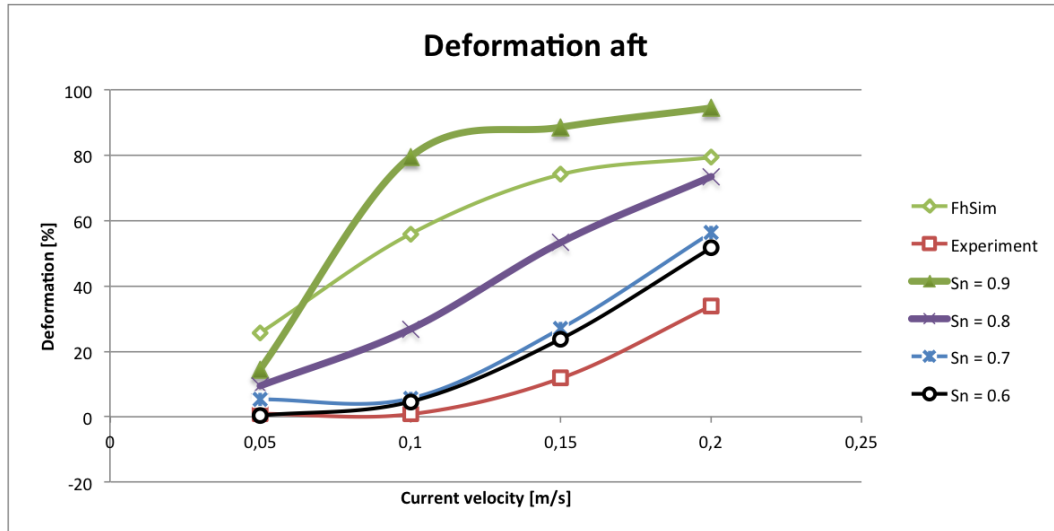


Figure 3.9: Deformation on the aft part of the skirt attached to the net cage.  $Sn = 0.9$  to 0.6 indicates the varying solidity in AquaSim. Both FhSim calculation and experimental test values was obtained with  $Sn=1$ .

Deformation at the aft position of the skirt is shown in figure 3.9. It is seen that there is small difference between  $Sn = 1$  (fig. 3.6) and  $Sn = 0.9$  (fig. 3.9). However, a solidity reduction to 0.8 gives significant reduction in the deformation. The difference between  $Sn = 0.7$  and 0.6 is small, but follow the same pattern for increasing velocity as the values obtained in the experiment. There is overestimation for all of the AquaSim values compared with the experiment in Hirtshals. A solidity of 0.9 will also give larger deformation when compared with the simulation tool FhSim.

Based on these test trials, a solidity of 0.7 should be used in order to obtain accurate data. However, only one experiment has been used for comparison and the reduction in solidity may have different effects based on how the net cage is constructed. For capacity validation through analysis, a solidity of 0.8 would therefore be recommended as conservative results are obtained.

### 3.2.3 Skirt only

In order to investigate the effects of Permaskirt in greater detail, a model consisting only of the skirt and weights was made, neglecting the contribution from the net cage, sinker tube and ropes. This configuration was also examined by [Lien and Volent, 2012] and [Rundtop and Lien, 2013].

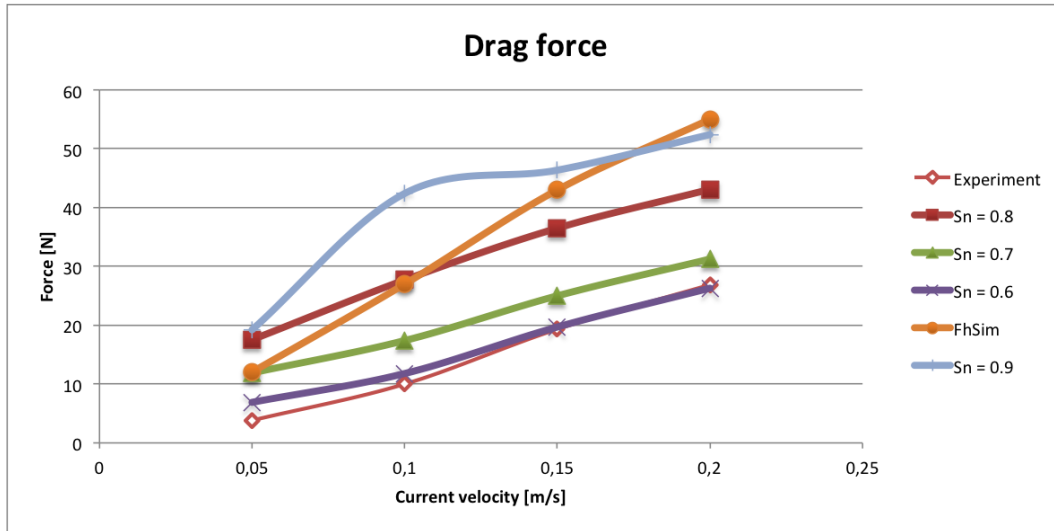


Figure 3.10: Drag force on the structure, with Permaskirt only.  $Sn = 0.9$  to  $0.6$  indicates the varying solidity in AquaSim. Both FhSim calculation and experimental test values was obtained with  $Sn=1$ .

Figure 3.10 shows the drag force on the structure with varying solidity from  $0.9$  to  $0.6$ . Results for  $Sn = 1$  with skirt only are found in figure 3.3. For  $Sn = 0.9$ , there is small difference when the current velocity is increased from  $0.1$  to  $0.15\text{m/s}$ , which differs from other test trials. There is also large deviation compared with experimental values.

As expected, the drag force is reduced for reduction in solidity. However, it is seen that the solidity needs to be reduced to  $0.6$  to obtain similar values as the measured ones. For the case with full configuration, a reduction to  $Sn = 0.7$  was adequate in order to obtain similar results.

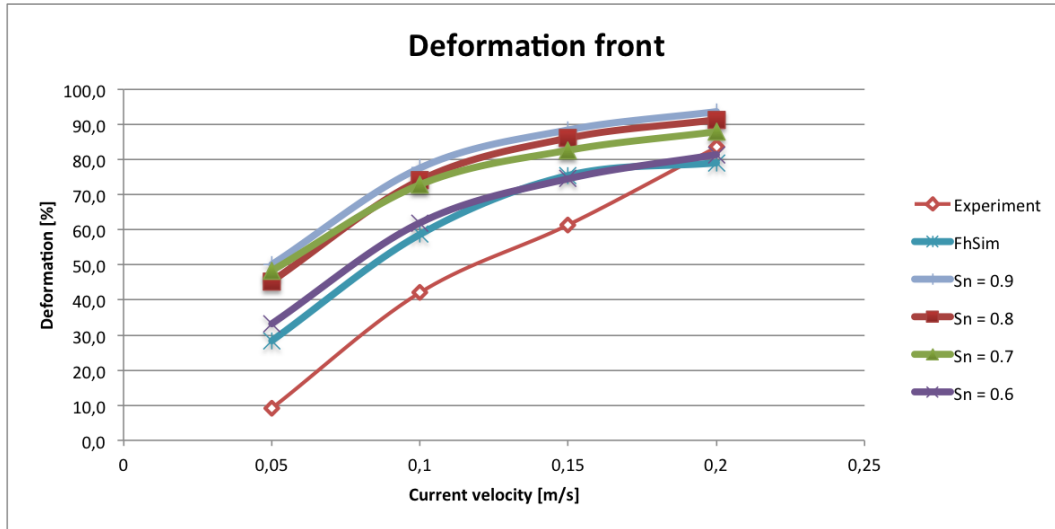


Figure 3.11: Deformation on the fore part of the skirt, for the case with skirt only.  $Sn = 0.9$  to  $0.6$  indicates the varying solidity in AquaSim. Both FhSim calculation and experimental test values was obtained with  $Sn=1$ .

Deformation at the fore part of the skirt is shown in figure 3.11. It shows small differences for  $Sn = 0.9, 0.8$  and  $0.7$ . Noticeable reduction in deformation is first obtained for  $Sn = 0.6$  which are of about the same deformation values as calculated by FhSim. It is seen that the largest deviation for all test trials, compared with experimental values, is for the lower current velocities. For  $U = 0.2m/s$  most of the values are at about 85% deformation.

At the aft position of the skirt, figure 3.12, there are large differences for the different solidity ratios. From large overestimation at  $Sn = 0.9$  to almost no deformation at  $Sn = 0.7$ . The different solidity calculations show that the choice of solidity has a large effect for the aft deformation and should be used with care. FhSim also over estimates the deformation, compared with experimental values.



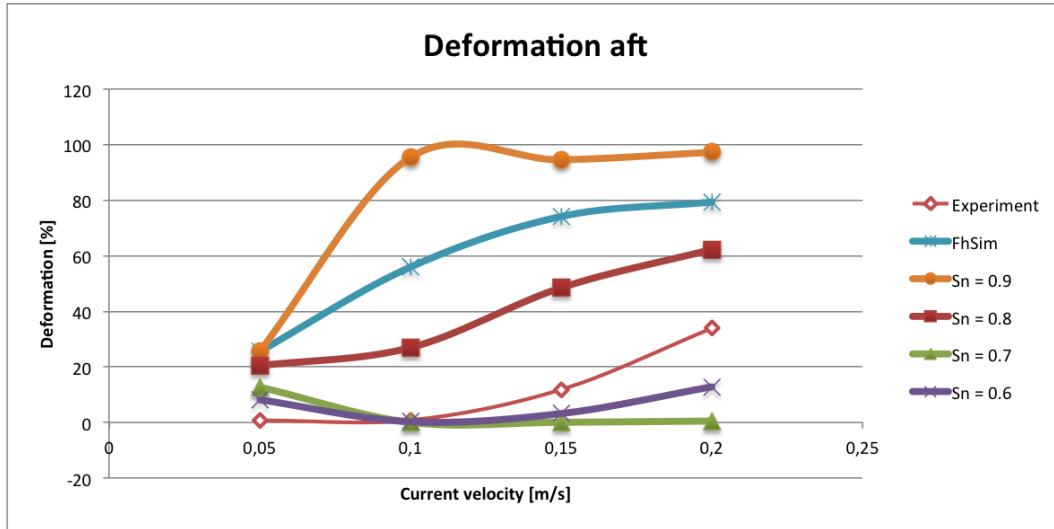


Figure 3.12: Deformation on the fore part of the skirt, for the case with skirt only.  $Sn = 0.9$  to  $0.6$  indicates the varying solidity in AquaSim. Both FhSim calculation and experimental test values was obtained with  $Sn=1$ .

By neglecting the net cage, the effects of the skirt are easier to investigate. At the aft position, AquaSim calculations show almost no deformation for  $Sn = 0.7$  and  $0.6$ .

In the fore part of the skirt, the deformation seems independent of solidity for  $Sn = 0.9$  to  $0.7$ . For a skirt only simulation, suggested solidity would therefore be  $0.6$ , which differs from the case with full configuration. This shows that a reduction in solidity for the whole skirt may not be the best method to obtain proper results, since suggested solidity depends on the configuration.

### 3.2.4 Locally varying solidity

In order to obtain more accurate and dependable results from AquaSim, the net was split into different panels and each panel was given a local solidity. The skirt was divided vertically into 36 different panels and test trials with both full configuration and skirt only was performed.

Based on the pressure distribution in figure 3.2, the local solidity was set. Since the calculated pressure distribution only were calculated for  $0 < \theta < 90deg$ , symmetrical properties fore and aft were assumed in order to obtain values for the aft part of the skirt where  $\theta > 90degrees$ . Left and right symmetry was also assumed.

The pressure in AquaSim was extracted by dividing the force,  $F$ , on the projected area,  $A_p$ , of a twine element. Figure 3.2 shows that calculated pressure in AquaSim was about half of the other two methods at the stagnation point. The foremost panels should therefore have been given a much higher solidity in order to increase the pressure in AquaSim. Different trials with high solidity (larger than 1) panels on the fore side were performed, but both drag force and deformation were highly overestimated compared with experimental data.

Since deformation is an important parameter for skirt calculations, it was decided to reduce the solidity of the fore and aft panels to 0.5 in order to obtain good estimations for skirt deformation. A solidity of 0.5 for the foremost panels was chosen based on the trial and error method.

The force distribution, which the pressure distribution was based on, gave an almost linear decrease from  $\theta = 0$  to  $\theta = 90$ . The solidity of the skirt panels was therefore varied linearly from  $Sn = 0.5$  to 1.1 in order to obtain accurate results for both drag force and deformation. A solidity of 1.1 is not physical, but the formulation in AquaSim allows it to be used. The lowest solidity was given for the fore and aft panels ( $\theta = 0$  and  $180deg$ ), while maximum solidity was chosen for the side panels ( $\theta = 90$  and  $270deg$ ). High solidity panels on the side panels increased the total drag force and were therefore important to obtain correct drag force on the structure.

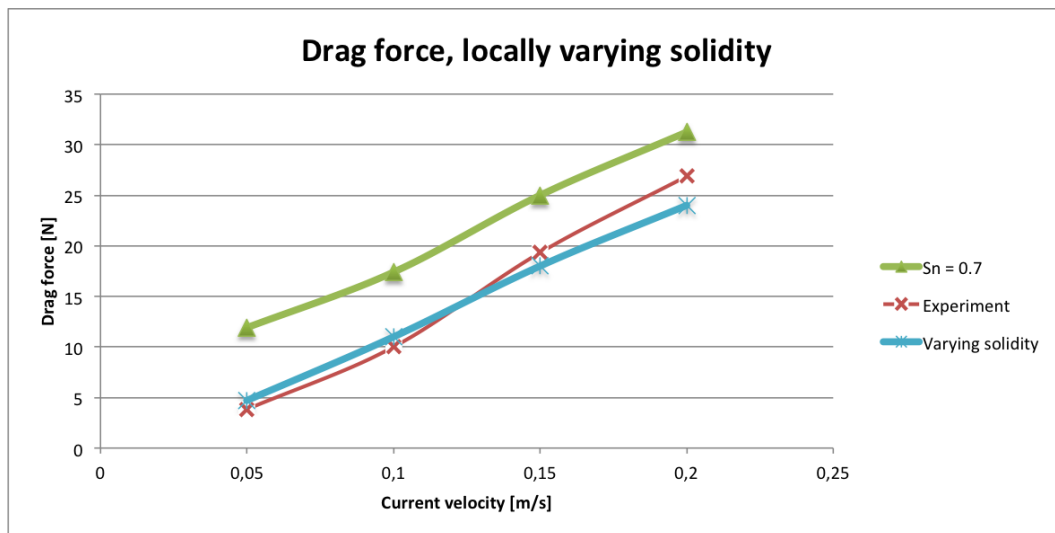


Figure 3.13: Drag force on the construction with only the skirt attached to the floating tubes. "Sn = 0.7" indicates the case with a uniform solidity of 0.7 calculated in AquaSim. "Experiment" is the values obtained in Hirtshals, and "Varying solidity" indicates the case discussed in this chapter.

The average solidity for the panels with different solidity was 0.74 and the drag force for a uniform  $Sn = 0.7$  was included in figure 3.13. As seen from the figure, good results are obtained from the method of locally varying solidity. Largest deviation is found for  $U = 0.2\text{m/s}$  where there is a 10.7% underestimation. Compared with a uniform solidity of 0.7, it is seen that a varying solidity gives a better representation of the drag force on the skirt.

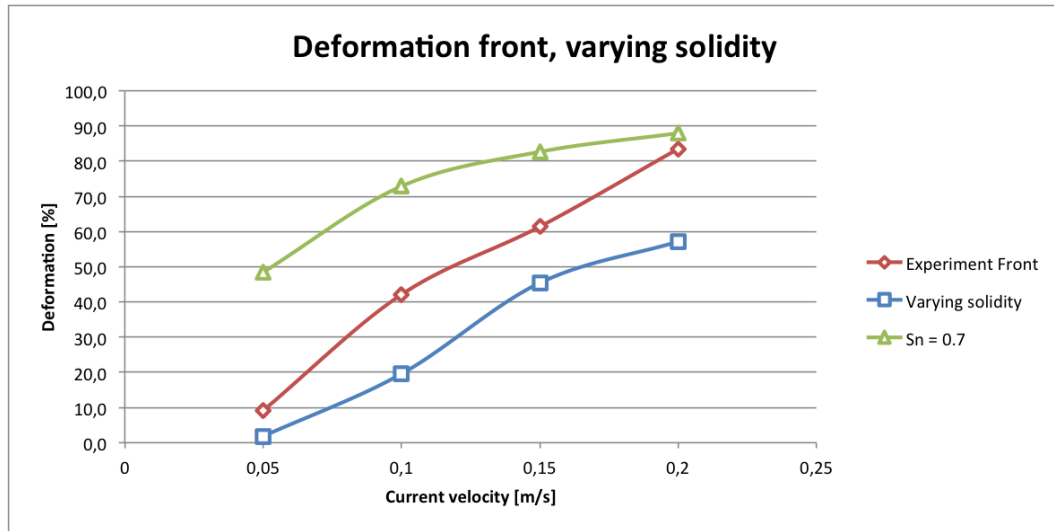


Figure 3.14: Deformation on the fore part of the skirt. "Sn = 0.7" indicates the case with a uniform solidity of 0.7 calculated in AquaSim. "Experiment" is the values obtained in Hirtshals, and "Varying solidity" indicates the case discussed in this chapter.

Figure 3.14 shows the deformation at fore part of the skirt. The use of varying solidity clearly reduces the deformation, and underestimated the deformation for all current velocities. For 0.2 m/s, the deviation is 46%. This underestimation is probably due to the low solidity at the foremost panels, causing small forces which leads to small deformations.

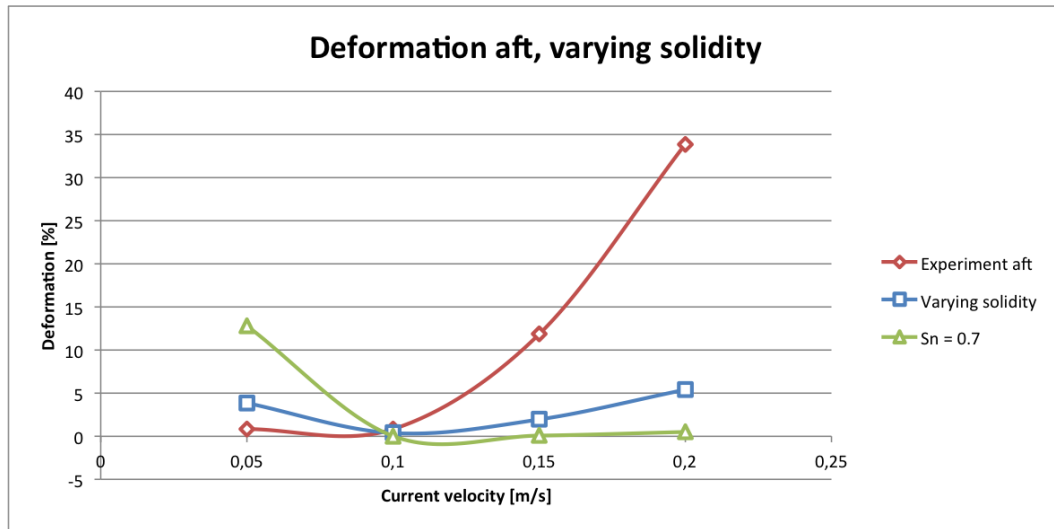


Figure 3.15: Deformation on the aft part of the skirt. "Sn = 0.7" indicates the case with a uniform solidity of 0.7 calculated in AquaSim. "Experiment" is the values obtained in Hirtshals, and "Varying solidity" indicates the case discussed in this chapter.

Deformation at the aft position of the skirt is shown in figure 3.15 and shows underestimation for higher current velocities compared with experimental values. Compared with the uniform case, the varying solidity case gives a better representation of the deformation when compared with the values obtained in Hirtshals. However, both fore and aft deformation are underestimated for this case when comparing with experimental values, and an increase in solidity for the fore and aft panels should be used for this case.

A skirt with varying solidity was also tested for the full configuration setup. The skirt was modelled exactly as for the "skirt only" trial, but net cage, sinker tube and connecting ropes was also added to represent the full configuration.

The calculated drag force for the net cage with skirt is presented in figure 3.16. The plot shows that there is some underestimation compared with experimental values. Maximum deviation, obtained at  $0.15\text{m/s}$ , is 12.25%. For the configuration with skirt only, the drag force was only underestimated for higher current velocities. While in full configuration, all current velocities gave underestimation.

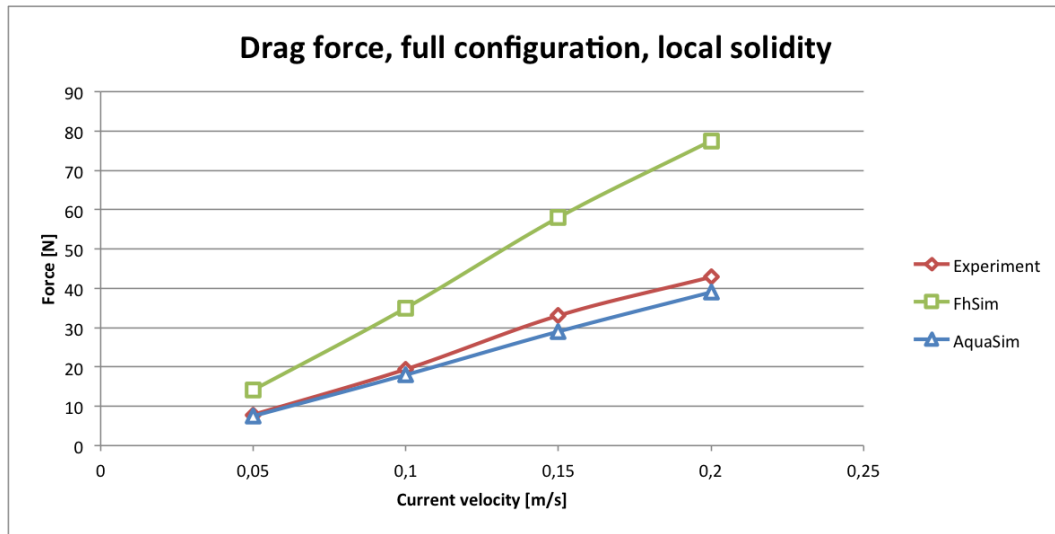


Figure 3.16: Drag force computed by AquaSim, compared with calculations executed by FhSim and experimental data. AquaSim had full net cage configuration with locally varying solidity for the skirt.

Deformation at the fore side of the skirt (fig. 3.17) shows underestimation, compared with experimental values, for  $0.05\text{m/s}$  and overestimates for larger current velocities. At  $0.05\text{m/s}$  the deformation, or rise in vertical direction, is only  $0.82\%$  of initial skirt depth.

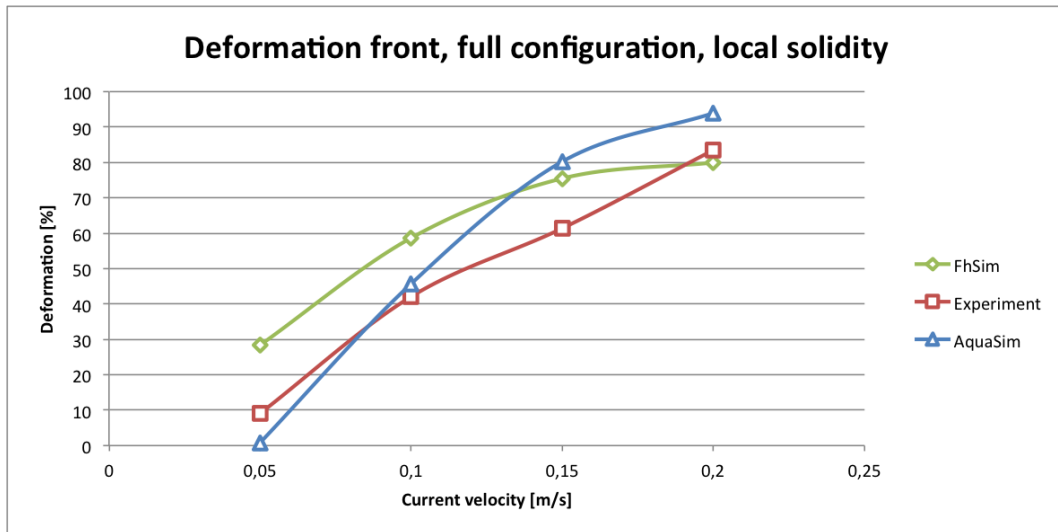


Figure 3.17: Deformation at the fore side of the skirt. AquaSim had full net cage configuration with locally varying solidity for the skirt.

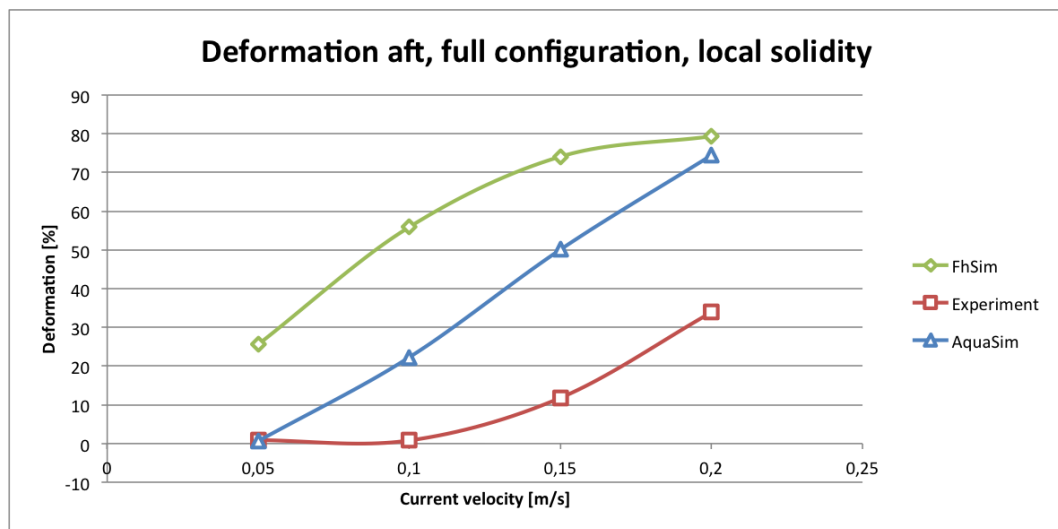


Figure 3.18: Deformation at the aft side of the skirt. AquaSim had full net cage configuration with locally varying solidity for the skirt.

Figure 3.18 shows the deformation at the aft position at the skirt. At  $0.05m/s$  calculates only 0.64% deformation which is similar to the experimental values. For increasing current velocity, there is overestimation.

The two plots (fig. 3.17 and 3.18) shows that there is underestimation for  $0.05m/s$  and then overestimation for larger current velocities. Comparing this with figure 3.16 it is seen that for the cases with overestimated deformation, as expected, the drag force is underestimated.

For the skirt only configuration, the calculations with locally varying solidity were compared against uniform solidity for the skirt. Except for the deformation at the fore part of the skirt, the locally varying solidity gave better results than the uniform case compared against experimental values.

When the locally varying solidity skirt was added to the net cage in full configuration, good results were obtained. The aft deformation was higher than what was measured in the experiment, probably due to water flowing through the skirt, increasing the force on the aft part of the skirt.

In general were good results obtained with a varying solidity skirt in full configuration. Comparison of pressure distribution alone in order to adjust the local solidity, gave large overestimations for both drag force and deformations. It was therefore decided to combine the pressure distribution with deformation results for a skirt with uniform solidity. The results presented in this chapter are a result of this combination.

There are large differences in how well the simulated results coincide with experimental data for the two different setups. This implies that it is difficult to develop one method that will work for different configurations. Different factors, such as pressure and deformations, should be accounted for. More experimental data would therefore be preferable in order to check if the method with varying solidity gives good representation of drag force and deformation for other full configuration setups.

### 3.3 CFD results

For this thesis, CFD calculations has been performed with the simulation tool Ansys Fluid in order to find both pressure distribution around a skirt without deformation, as well as the flow distribution around and inside the deformed skirt.

#### 3.3.1 Pressure distribution

One of the proposed methods to evaluate the local solidity around a Permaskirt, was to look at the pressure distribution. Potential flow theory was used for hand calculation, but due to many assumptions may this theory may give incorrect pressure values. CFD calculation is therefore a good solution when a greater accuracy in pressure distribution is desired.

Since the calculations in both potential flow theory and AquaSim consisted of a rigid cylinder without deformation, a similar model was made in Ansys. Geometrical values were the same as used for the other methods, and are explained in chapter 3.1. Results are plotted in table 3.2. Note that these comparative pressure calculations had a current velocity of  $0.2m/s$ , while further CFD calculations had  $U = 0.1m/s$ .

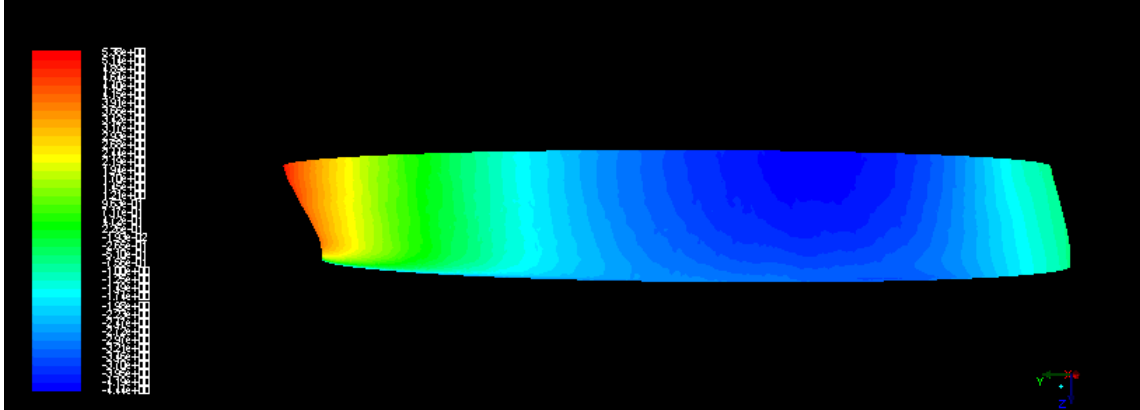


Figure 3.19: Pressure distribution on the deformed skirt, seen from the left, at  $U = 0.1m/s$ . Maximum pressure is 5.38 Pa and minimum is -4.43 Pa.

Figure 3.19 shows the pressure distribution on the deformed skirt as calculated in Ansys Fluid. Maximum pressure is obtained at the front panels, near the free surface. Due to the deformation, the incoming current is led down under the skirt, reducing the pressure on the net as the depth is increased.



### 3.3.2 Velocity distribution

The idea behind a Permaskirt is to stop the upper layers of water flowing through the net cage. However, water containing lice may be pushed down under the skirt and enter inside the skirt. An investigation regarding flow distribution for a skirt, is therefore of interest.

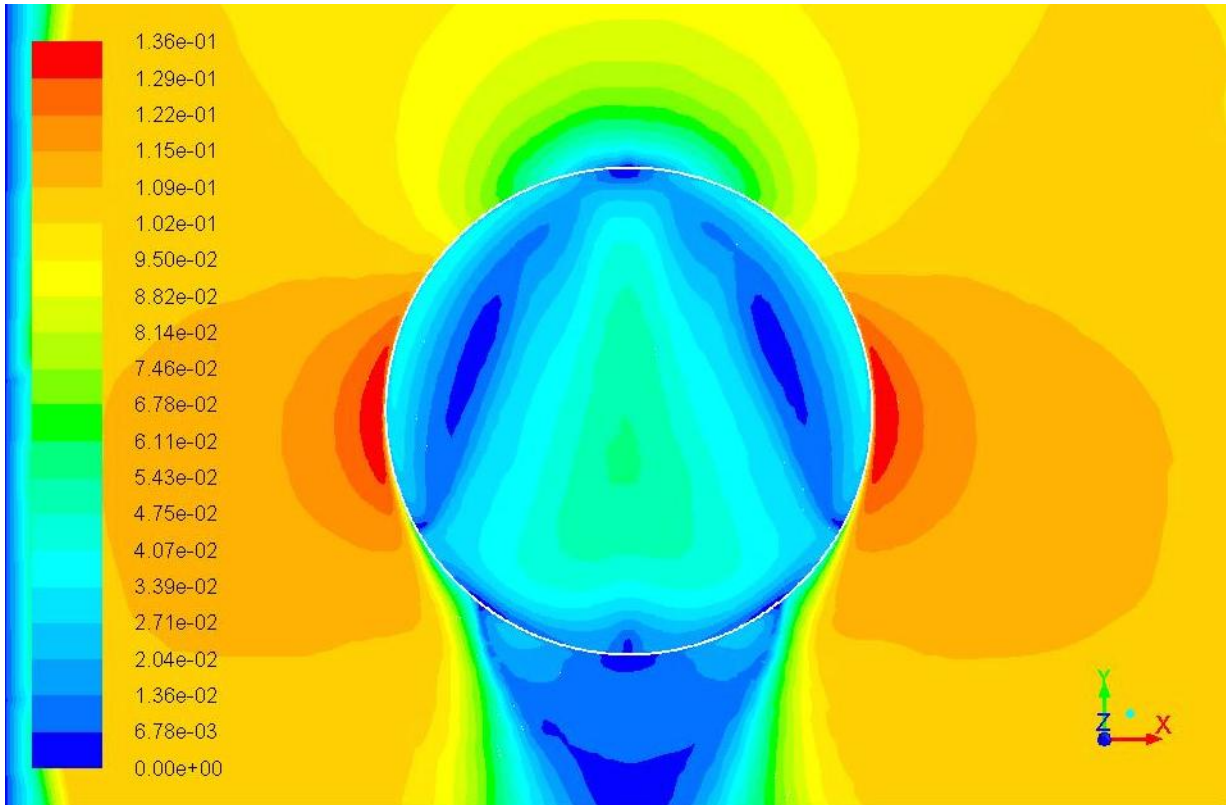


Figure 3.20: Contour plot of the velocity distribution at the free surface. The velocity is in  $m/s$ .

Figure 3.20 and 3.21 shows the velocity distribution at the free surface. Physically expected phenomena, such as reduced velocity at stagnation point and maximum velocity at the sides, are observed.

Inside the skirt, a triangular pattern is observed (fig. 3.20). The largest velocity inside the skirt is found at the center, with most of the particles traveling against the undisturbed current direction.

As seen on figure 3.21, most of the current traveling at the free surface will be directed around the skirt.

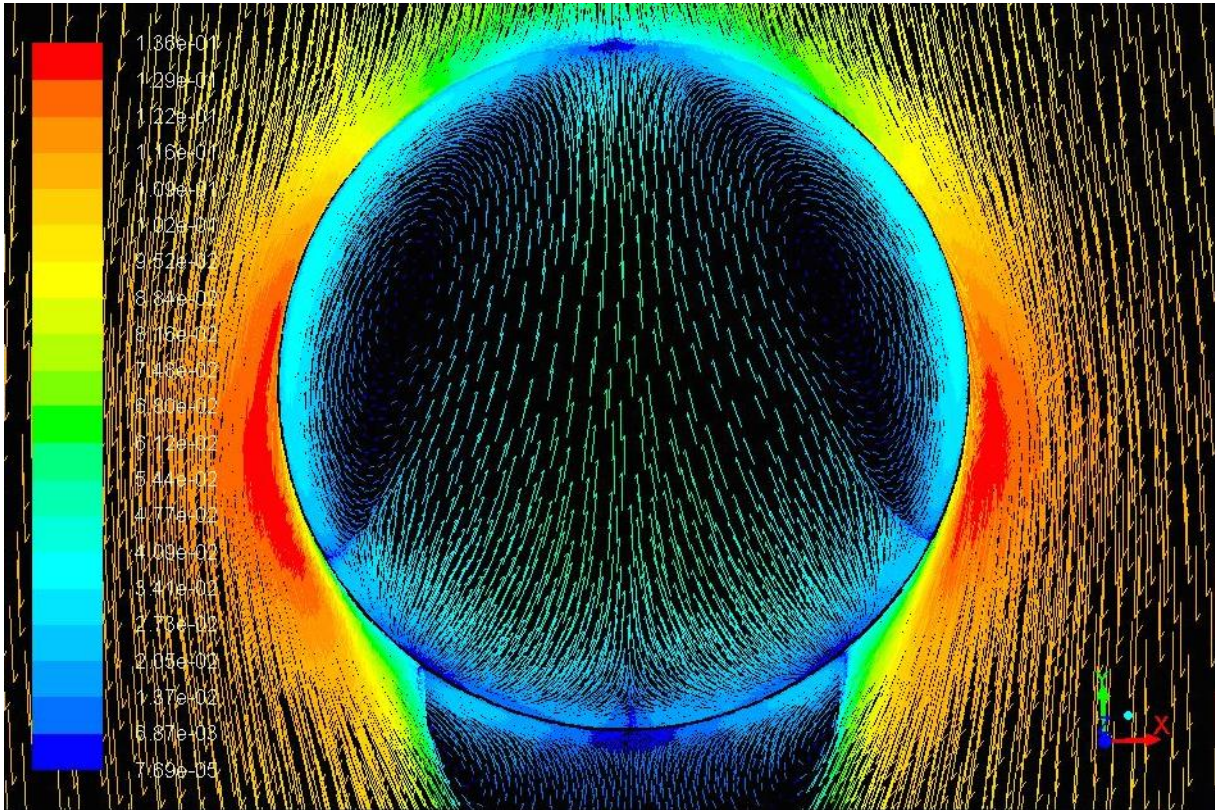


Figure 3.21: Vector plot of the velocity distribution at the free surface. Note that the water inside of the skirt travels in opposite direction of the undisturbed current. The colorbar is difficult to read, but it is the same as for figure 3.20.

Figure 3.22 and 3.23 shows the velocity distribution in the vertical plane. It is observed how the water get pushed down and under the skirt, increasing the velocity. The current passing under the skirt accelerates the water inside the skirt, causing it to move in a circular motion.

The water particles, which are pushed under the skirt, may cause the lice to attach to the fish at a larger depth than normally experienced. This is investigated further in chapter 3.3.4

Since the largest current velocities under the skirt are at the center, the triangular pattern observed in figure 3.20 appears.

The contour plot (fig. 3.22) shows that there will be increased current velocity in the area between the skirt and tank bottom. Later in this chapter, the effects of tank bottom depth are therefore investigated.

It is also observed that the skirt will influence the ambient flow. For a fish farm with many net cages fitted with Permaskirt close to each other, these changes in flow distribution would probably influence the forces on succeeding net cages.

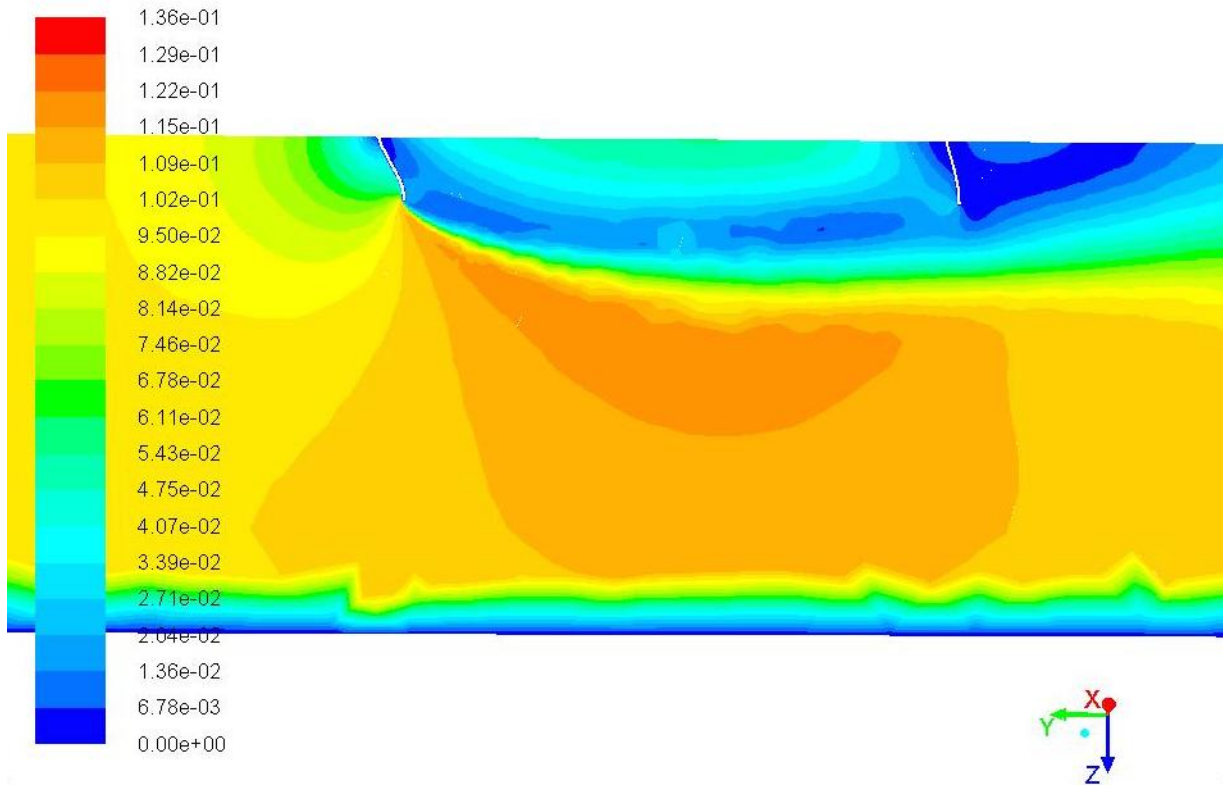


Figure 3.22: Contour plot of the velocity distribution in the vertical plane.

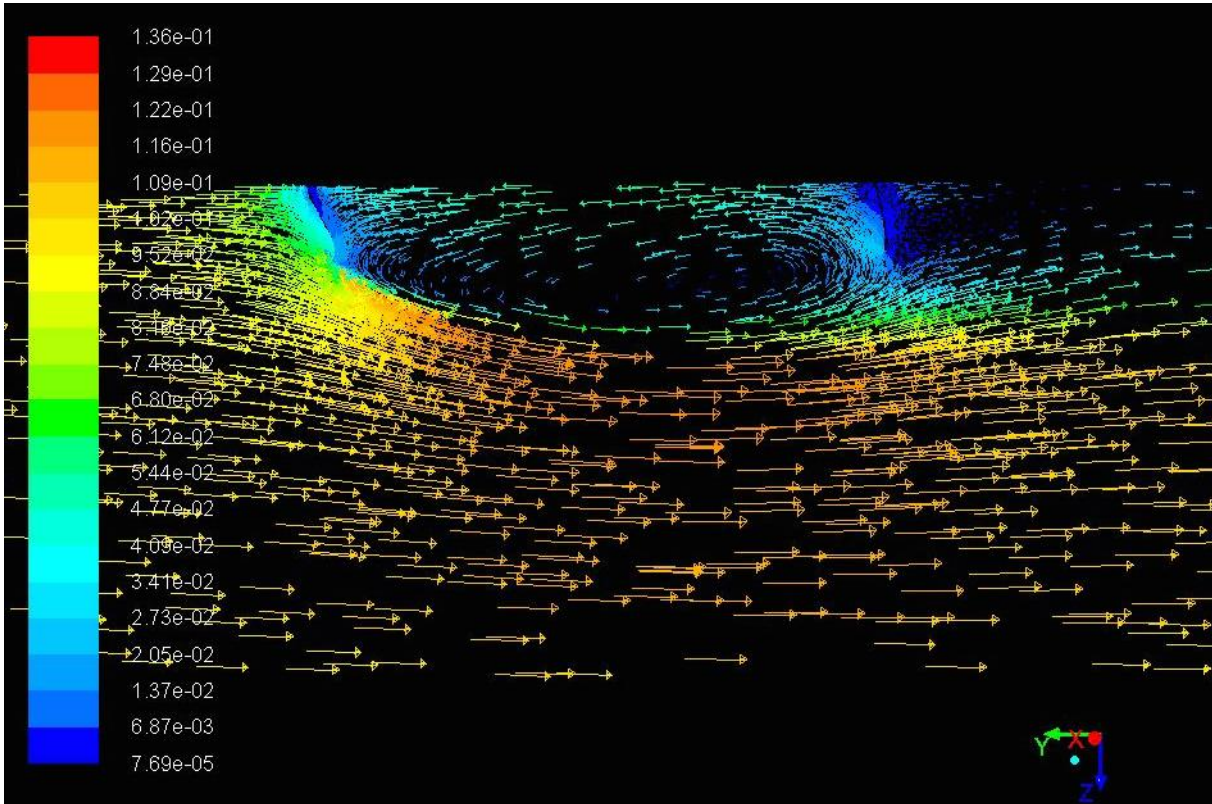


Figure 3.23: Vector plot of the velocity distribution in the vertical plane.

### 3.3.3 Comparison with measured data

The experiment in Hirtshals also included velocity measurements in and around the skirt [Lien and Volent, 2012]. Five electromagnetic sensors were placed 5cm below the free surface and placed as shown in figure 3.24. The first sensor (position 1) was placed in front of the skirt, towards the incoming current. Position 2, 3 and 4 was inside the skirt while position 5 was placed downstream of the skirt.

The sensors were oriented with axes in the normal and transverse direction with respect to the incoming current, making it possible to measure both magnitude and direction of the local flow.

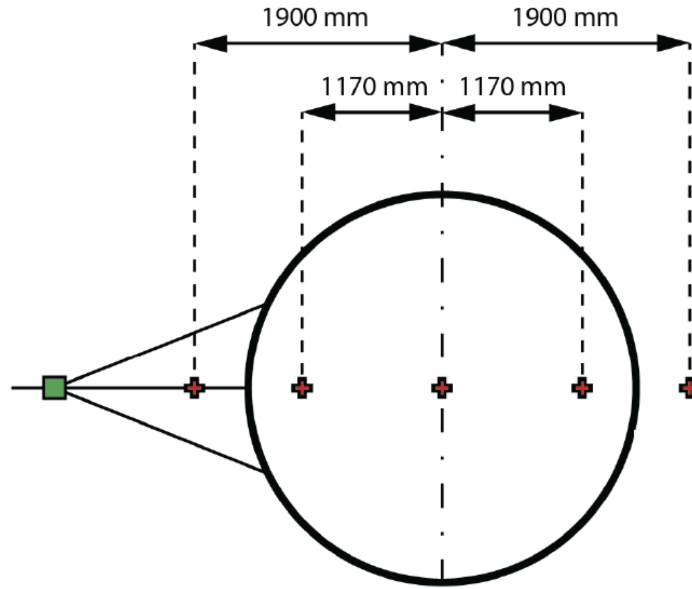


Figure 3.24: Placement of electromagnetic velocity sensors in the experiment. Green box indicates load cell for drag force, while red crosses indicates velocity sensors. Courtesy: [Lien and Volent, 2012].

Comparison of flow velocity and direction, between CFD analysis and experimental values, are presented in figure 3.25. Each plot represents the flow velocity and direction for a point presented in figure 3.24.

Figure 3.25a shows the current velocity and displacement for position 1, 1.9 meters from the center in the upstream direction. The simulated direction vector shows good similarity with experimental values, while the velocity has some underestimation.

At position 2, fig. 3.25b, which is placed inside the skirt upstream from center, the velocity is overestimated. Simulations give flow direction in the negative direction.

Figure 3.25c presents the magnitude and direction of the flow at the center of the skirt. Some overestimation regarding the flow velocity is also observed here. Simulated direction shows a good representation compared with experimental values.

At position 4, fig. 3.25d, both simulated flow velocity and direction vector gives fairly good results compared with measured values.

At the downstream point, outside the skirt, fig. 3.25e, some underestimation is observed for flow velocity. Simulation gives a flow direction in the negative direction.

The simulations in Ansys Fluid were time averaged, while measured values were time dependent. For some locations, such a position 2, there is a large scattering in measured

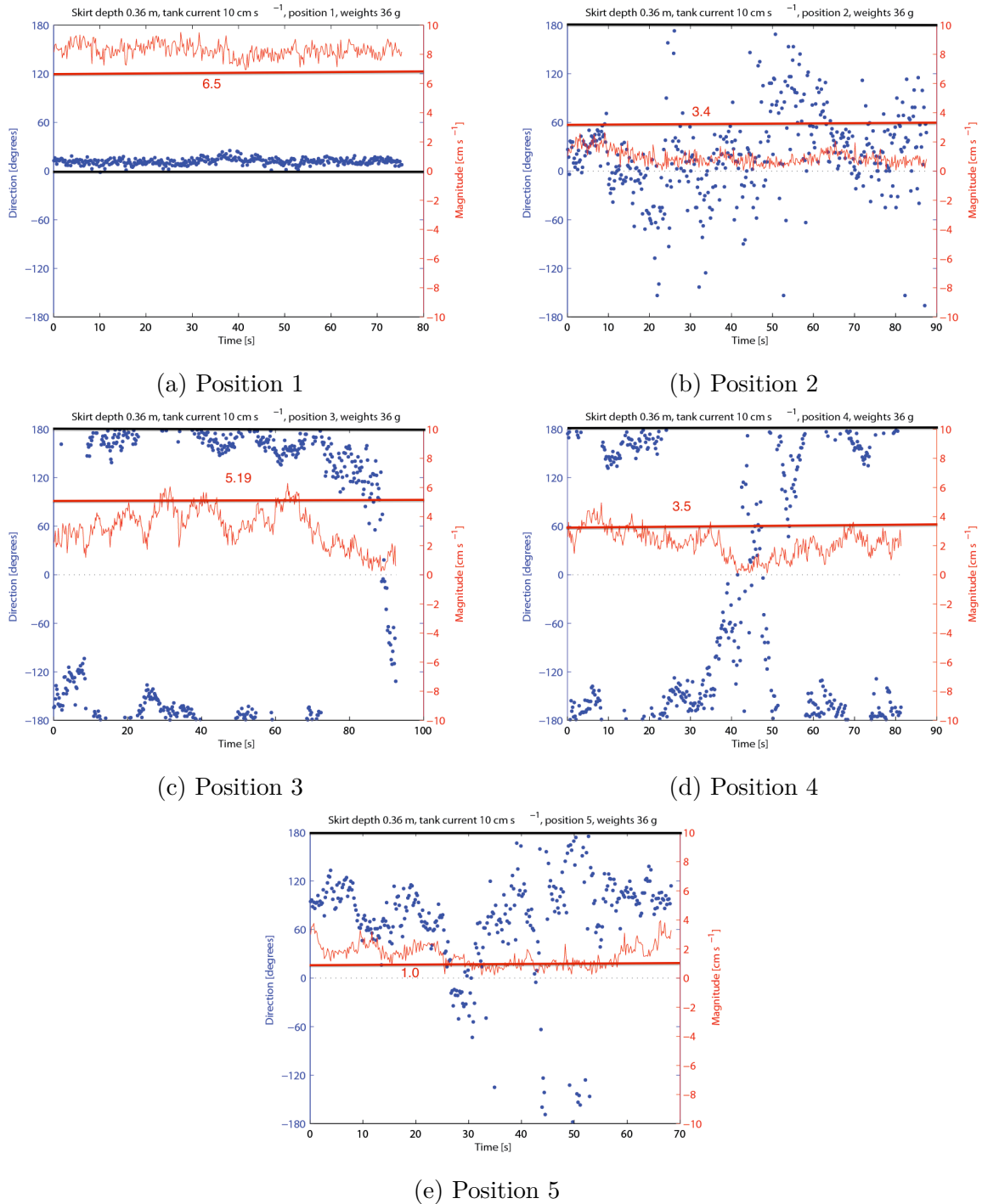


Figure 3.25: Comparison of flow velocity and direction between CFD simulation and experiment for five different positions. Blue dots indicate direction [deg] and thin red line indicates magnitude of current [cm/s] in the experiment. Thick red line indicates simulated current velocity and thick black line indicates simulated direction. 0 degrees indicates free current direction, while 180 degrees indicates velocity against the undisturbed current.

flow direction. Implying that a time averaged simulation may not give accurate results.

Velocity calculations were in general higher than the experimental values at the inside of the skirt, while they were underestimated at position 1 and 5, which were located outside of the skirt. In position 5, irregular flow pattern is expected. Correct results in a time averaged simulation will therefore be difficult to obtain.

In general, the simulation showed good results when compared with experimental values. CFD seems to be a good method in order to predict the flow distribution in and around a skirt. However, good knowledge about the deformation pattern of the skirt must be obtained. This thesis uses therefore both AquaSim and Ansys Fluid together to obtain the final results.

### 3.3.4 Estimated effect of PermaSkirt, based on CFD analysis

As seen from figure 3.23, water approaching the skirt will be pushed down and under the skirt, causing rotation of the water inside the skirt. If the incoming current, carrying lice, travels inside the skirt after being pushed under, lice would be able to enter the volume limited by the skirt.

In order to investigate this problem, ten CFD computations was initiated and number of streamlines entering the skirt was counted in the post processing of each file.

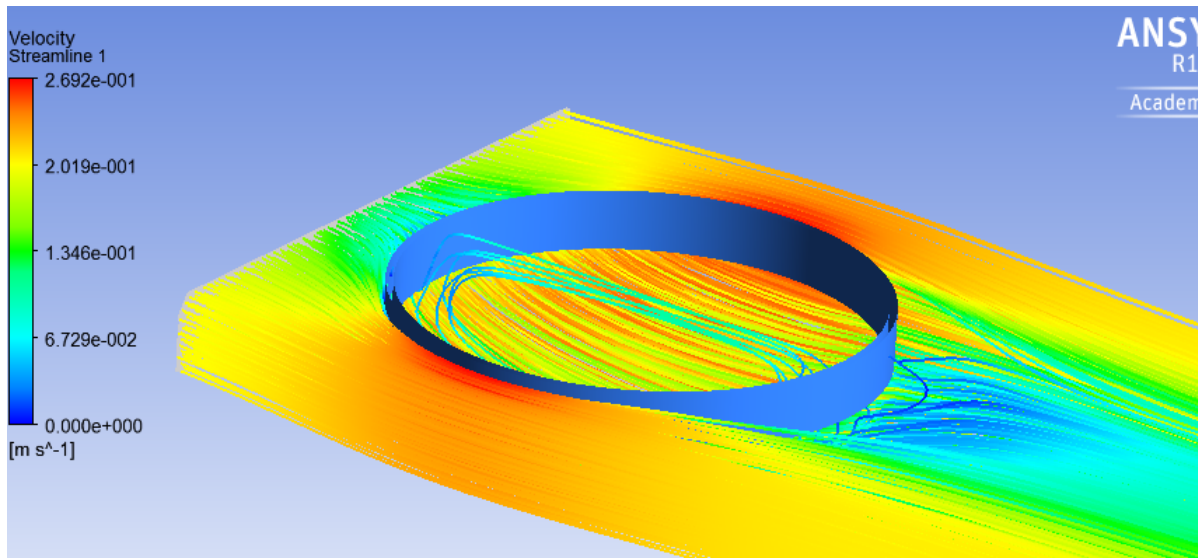


Figure 3.26: Isometric view of the streamlines used for calculating the number of particles entering the volume limited by the skirt. For this case, 2/1000 of the streamlines projected from the plane in front of the skirt were circulated inside the skirts volume.

Figure 3.26 shows how the counting was performed. In the post processing, a plane with a depth of  $1m$  and a width of  $4m$  was placed  $0.5$  meters in front of the foremost panel. From this plane, 1000 streamlines were projected and the number of streamlines entering inside the skirt was counted. As this was a time averaged simulation, pathlines, streamlines and streaklines would match.

The ten different simulations showed that 0.39% of the streamlines projected from the plane went into the volume limited by the skirt. By assuming full streamline penetration through a regular net cage, it is clearly seen how effective the use of Permaskirt may be. However, [Næs et al., 2012] investigated the reduction on lice in full scale. Results from that experiment showed that Permaskirt reduced the number of lice with a factor of 4.



Based on CFD results, this factor should be larger. However, the skirt in the full scale experiment was not completely watertight in order to assure sufficient oxygen level in the net cage and reduce the forces on the structure. This effect was not investigated in the project, but it is a mentioned error source that should be taken into account.

When looking at figure 3.26, it is observed that a large number of pathlines are pushed down and under the skirt. For a net cage in operating condition, these pathlines would run through the net cage, causing lice to attach to the fish at a deeper depth than normally experienced. The density of lice in the surrounding environment around the net cage and how easy they attach to the fish will also be of importance, but this has not been investigated in this thesis. Increase in current velocity below the skirt is observed, this may decrease the number of lice attaching to the fish, since the lice will spend a shorter time inside the net cage.

In full scale operation condition, the waves will also be of concern when calculating the effect of Permaskirt. For a skirt with the upper edge at the free surface, waves may go over the skirt, causing lice to enter the volume of the net cage protected by the skirt. This effect has not been investigated by this thesis, but an increase in skirt height over the free surface will probably be a good solution.

A possible solution to reduce the number of water particles entering inside the skirt would be to increase the depth of the skirt. This would lead more of the flow from the upper layers, containing lice, to go around the skirt instead of being pushed under it. However, a larger skirt would increase the forces on the structure and probably reduce the oxygen level inside the net cage, which could harm both the structure and the fish. In order to decrease the forces on the structure and assure sufficient oxygen level for a deeper skirt, a skirt that is not completely watertight may be used. [Næs et al., 2012] had a skirt with  $0.35\text{mm}$  mask width, which was probably too large for full blocking effect against the lice. However, the measured oxygen inside the net was satisfying, implying that the mask width may be reduced without compromising the fish welfare.

CFD calculations with non deformed skirt showed that more streamlines were traveling around the skirt, instead of going underneath. This is because the deformed skirt creates an inclined wall at the foremost part, causing the water to travel this path instead of being pushed around the skirt. Based on these observations, Permaskirt should be mounted with sufficient weights in order to reduce deformation. As seen from previous calculation in AquaSim, reduced deformation of the net will increase the drag force on the structure. This would lead to a greater demand in proper calculation methods before installation in order to prevent structural failure.

### 3.3.5 Increased depth

The tank in Hirtshals had a depth of  $2.7m$ , which gives a full scale depth ( $\lambda = 17$ ) of  $45.9m$ . In order to see how the depth of the tank influenced the flow distribution, a CFD analysis with  $5.4m$  tank depth was performed.

The flow distribution, presented as pathlines in the vertical plane is shown in figure 3.27. Some reduction in current velocities, compared with figure 3.23 is observed.

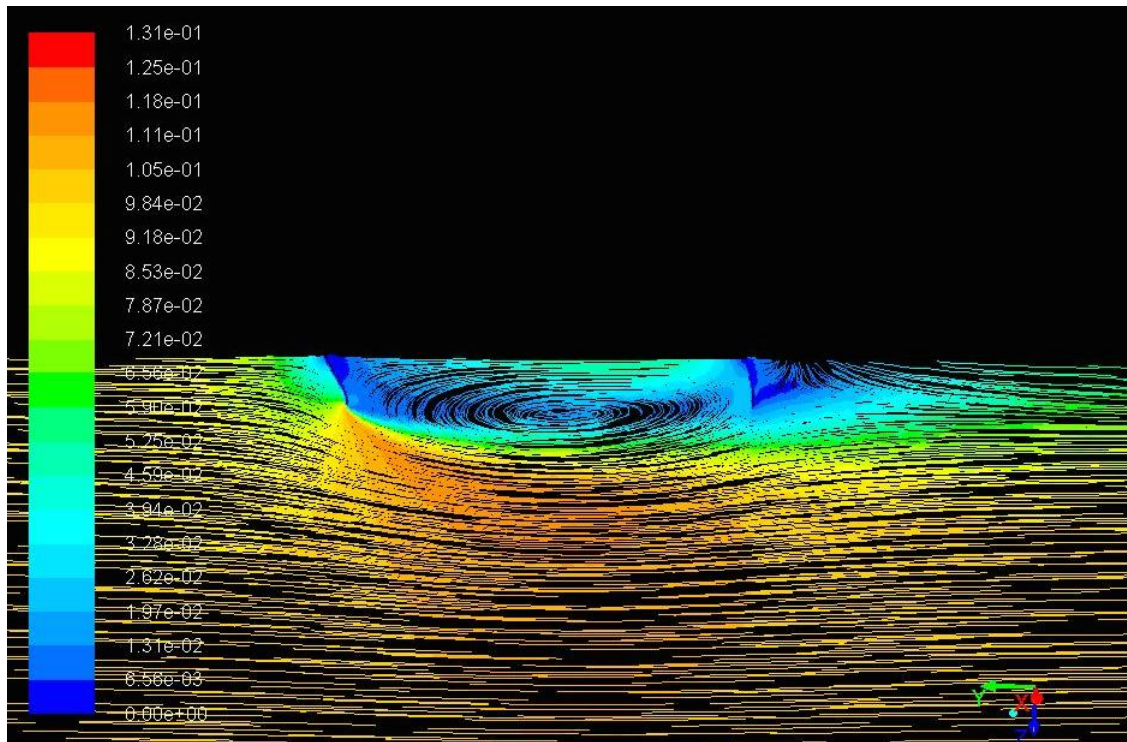


Figure 3.27: Flow distribution, displayed as path lines with a tank depth of  $5.4m$ . Color bar shows the velocity in  $m/s$ .

Figure 3.28 shows a plot for the current velocity as a function of depth for the same test conditions as used in the experiment. As seen from figure 3.23, there will be negative current velocities inside the skirt due to rotation of water.

The velocity distribution at the center of skirt is marked as the blue line in figure 3.28. At the free surface the velocity is  $-0.0533m/s$ . Further down, the flow velocity in positive direction will increase and exceed the undisturbed current velocity. Maximum velocity is  $0.12m/s$  at  $1.1m$  below the free surface, which is a 20% increase compared with the undisturbed current velocity.

5 meters in front of the skirt, the undisturbed current travels at a velocity of  $0.1\text{m/s}$ , only affected by friction against the tank bottom.

Behind the skirt, displayed as red line, there is still a reduction in velocity in the upper part of the tank, and an increase in velocity in the middle of the tank. For fish farms with many net cages behind each other, this reduced velocity should therefore be accounted for.

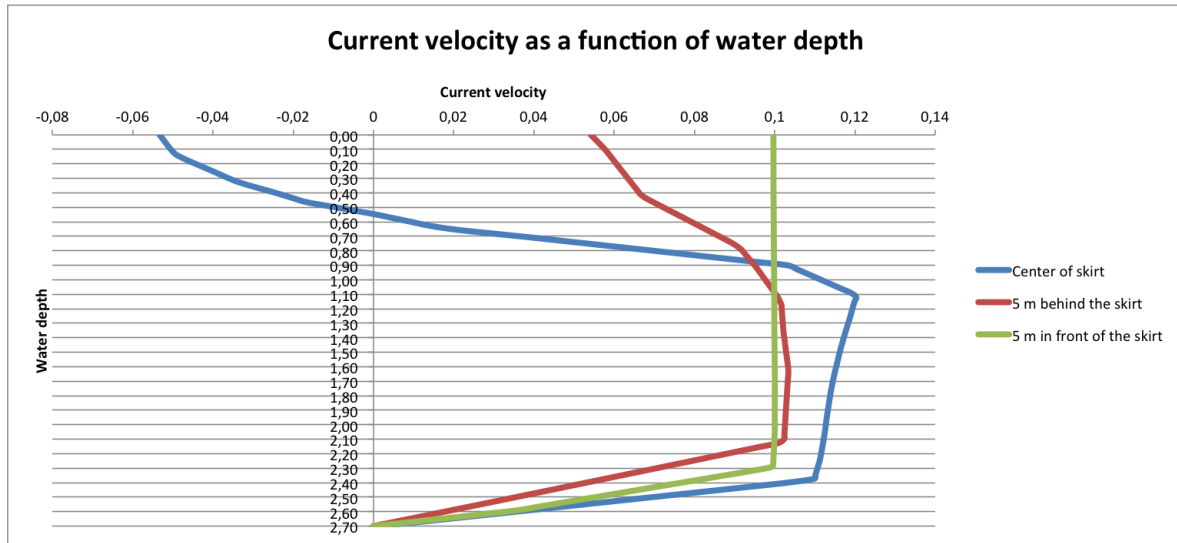


Figure 3.28: Current velocity as a function of depth. The velocity distribution is presented 5 meters in front of the skirt, 5 meters behind the skirt and at the center.

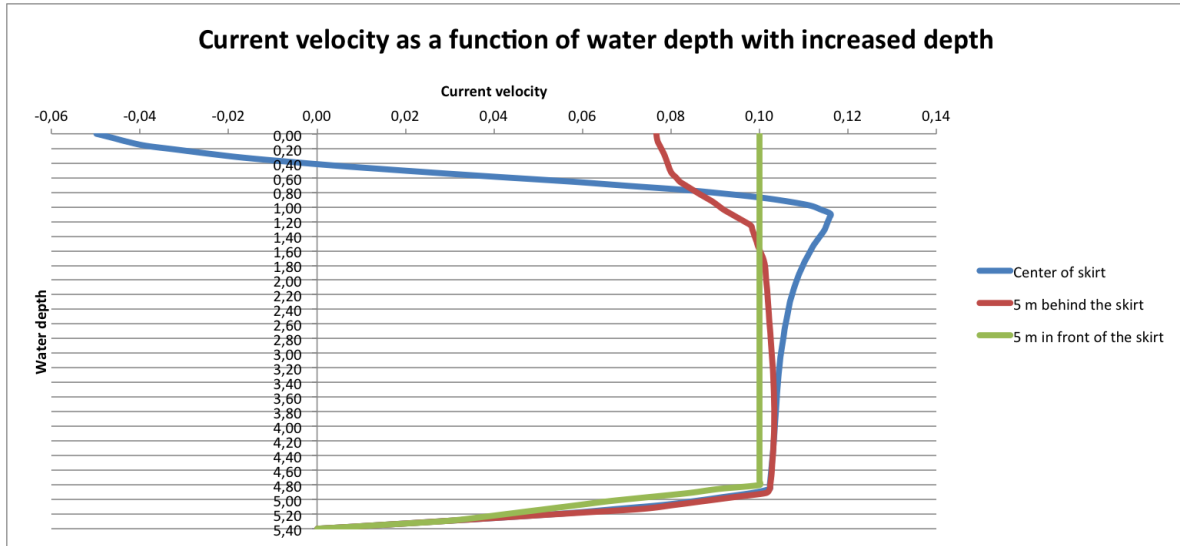


Figure 3.29: Current velocity as a function of depth with increased water depth. The velocity distribution is presented 5 meters in front of the skirt, 5 meters behind the skirt and at the center.

Results for the case with increased tank depth, is shown in figure 3.29. At the free surface, in the center of the skirt, there is a very small difference of only  $0.003\text{m/s}$  when comparing the two tank depths, where the case with tank depth of  $2.7\text{m}$  gives the highest velocity. This trend is seen for most of the velocity distribution at the center of the skirt.

The biggest difference is found for the velocity distribution 5 meters behind the skirt. Here, the free surface velocity is increased from  $0.054\text{m/s}$  to  $0.08\text{m/s}$  when the tank depth is doubled, giving it an increase of 48%. For several net cages, fitted with Permaskirt and placed behind each other, sea depth should be taken into account when calculating forces on succeeding net cages.

### 3.4 Error sources

In this thesis, different calculation methods have been compared with experimental measurements. Since most of the calculation methods have some assumptions, it is difficult to reproduce accurate data compared with experimental data. In this chapter, the error sources that are assumed to give larges deviation are discussed.

### 3.4.1 Deformation measurement

Using simulation tools, such as AquaSim and FhSim, in order to reproduce results obtained from experiments, showed in general overestimation for deformation values compared with experimental data.

A possible reason for the deviation at the fore part could be due to interaction effect between skirt and net, which were not accounted for. Pictures from the experiment in Hirtshals [Lien and Volent, 2012] showed that the fore part of the skirt was pushed against the net cage. This will give friction forces, which reduces the deformation of the skirt. The calculated deformation will therefore be determined by the mass of the weights attached to the skirt.

Deformation at the aft position of the skirt was in general also overestimated. One of the reasons for the overestimation is that the elements in this area are exposed to a larger current velocity compared with the experiment. The method used for calculating current velocity on succeeding nets has been explained previously and it has been shown that it does not give precise results for high solidity nets, such as a Permaskirt. The aft part of the skirt will therefore experience an overestimated current velocity, which increases the deformation.

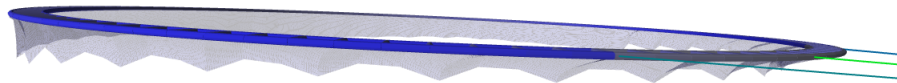


Figure 3.30: Isometric view of the skirt deformation in AquaSim.

The deformation in both AquaSim and FhSim was measured by taking the average of three nodes fore and aft of the skirt. Figure 3.30 shows the skirt deformation calculated by AquaSim for  $U = 0.2m/s$ .

Due to the deformation pattern caused by the weights attached to the skirt, the choice of nodes used for measurement will affect the deformation values. For this thesis and the modelling in AquaSim, the weights, or ropes, connecting the skirt with the sinker tube had connection points at the foremost and rearmost node. By selecting these nodes as the center of the three nodes used for measuring deformation, minimal deformation values would be measured.

This method was the same as used for the calculation in FhSim, while in the experiment the deformation was measured by using a camera. Different measuring methods

may therefore be an uncertainty in the compared results.

The skirt used in the experiment was made up by two skirt parts overlapping each other in order to make a full skirt. This meant that the fore and aft skirt could move independent of each other. In AquaSim, the skirt was modelled as one unit where deformation at the fore part would affect the aft part and vice versa.

### 3.4.2 CFD modelling

The deformed shape of the skirt used in CFD calculations was based on the deformation pattern calculated in Aquasim with  $Sn = 0.6$ . AquaSim was used since it was possible to extract three dimensional coordinates for each node, which could be imported into Ansys.

Due to difficult geometry, Ansys could not create surface between all node values. Therefore, the geometry had to be simplified and the curved net deformation between weights at the fore side of the skirt (fig. 3.30), had to be neglected.

By neglecting these deformations at the fore side of the skirt, the flow pattern will change. How much this would effect the simulated flow distribution has not been investigated in this thesis.

# Chapter 4

## Conclusion

This chapter concludes the thesis by a summary of the main findings. In addition, there are several aspects that should be considered for further work.

### 4.1 Conclusion

A Permaskirt fitted to a net cage will increase both forces and deformations on the structure. For this thesis, the simulation tool AquaSim, made by Aquastructures, has been used to investigate these effects. Results have been compared with results from experiment and the simulation tool FhSim. There has also been proposed a solution, with varying solidity of the skirt, to increase the accuracy of AquaSim simulations.

Initial calculations in Aquasim, with a skirt solidity of 1, showed that Aquasim highly overestimates both drag force and skirt deformation. As the skirt solidity was reduced, more accurate results, compared with experimental values, were obtained. The main reason for overestimation is due to the load formulation used in AquaSim, which is based on nets with a lower solidity.

Two different setups were investigated, one with skirt only and one with full net cage representing operating condition.

Reduction of skirt solidity gave reduction in both drag force and deformation. With a solidity between 0.6 and 0.7, good results were obtained with regard to both drag force and deformations. For capacity validation through analysis, a solidity of 0.8 would therefore be recommended, as conservative results are obtained.

In order to investigate the problem further, pressure distribution around the skirt was found with different methods and compared with AquaSim. Based on this distribution and deformation values, a skirt with varying solidity was modelled in AquaSim. The solidity was varied between 0.5 and 1.1, with an averaged solidity of 0.74. Simulated

results coincided good compared with experimental values.

In order to find pressure and flow distribution, CFD analysis was performed. Two different skirt models were tested, one without deformation and one with deformation.

Compliance between CFD analysis and experimental values were good, indicating that CFD analysis may be used to investigate the flow distribution around a net cage fitted with Permaskirt. However, good understanding of deformation pattern needs to be obtained. Combining simulation tools, such as Aquasim and Ansys Fluid or other similar programs, will therefore be preferable in order to obtain useful results.

Results obtained from CFD analysis showed that the incoming current was directed around and under the deformed skirt. Only a small part of the water entered inside the skirts volume.

Velocity distribution on the free surface showed that a maximum velocity of  $1.36m/s$  is obtained at the sides of the skirt, where  $\theta = 90deg$ , giving a velocity increase of 36%. In the vertical plane, maximum current velocity was found at the center of the skirt, 1.1 meters below the free surface and gave a 20% increase to the free current velocity.

Based on results from the simulations, mounting a skirt around a net cage could be an effective method in order to reduce spreading of lice. However, more information about the water particles passing under the skirt, and the risk of lice attaching to the fish at larger depth, should be obtained.

## 4.2 Recommendations for further work

Fish farming and methods to reduce the population of lice are increasing in popularity. Further work should therefore be performed in order to obtain more information and solutions to reduce lice in fish farming. In the following it is suggested several recommendations for further work:

- In order to improve the simulation results, load formulation for high solidity skirts should be developed together with methods taking into account contact between nets, and the occurring friction force.
- In order to get correct CFD results in full configuration, the effects of the net cage should also be included. For this thesis, only the effects of the skirt were investigated.
- Regarding CFD analysis in full scale, the effects of tank walls should be neglected by applying proper boundary conditions. In this thesis, only the effects of tank bottom depth were studied. It is observed that the skirt will influence the ambient flow. For a fish farm with many net cages fitted with Permaskirt close to each other, the effects of Permaskirt on the flow distribution should be investigated further.



# Bibliography

- [Aarsnes et al., 1989] Aarsnes, J., Løland, G., Rudi, H., and Åkre, H. (1989). Krefter og gjennomstrømning for merdsystem i strøm og bølger. Technical report, Marintek SINTEF-Gruppen.
- [Balash et al., 2009] Balash, C., Colbourne, B., Bose, N., and Rama-Nair, W. (2009). Aquaculture net drag force and asses mass. *Aquacultural Engineering*, 41:14–21.
- [Berstad, 2013] Berstad, A. (2013). *The AquaSim Package user manual*.
- [Berstad et al., 2012] Berstad, A., Heimstad, L., and Walaunet, J., editors (2012). *Loads from currents and waves on net structures*. Proceedings of the ASME 2012 31st International Conference on Ocean, Offshore and Arctic Engineering.
- [Berstad et al., 2004] Berstad, A., Tronstad, H., and Ytterland, A., editors (2004). *Design rules for marine fish farms in Norway. Calculation on the structural response of such flexible structures to verify structural integrity*. Proceedings of the OMAE 2004 23st International Conference on Offshore Mechanics and Artic Engineering.
- [Cebeci and Cousteix, 2005] Cebeci, T. and Cousteix, J. (2005). *Modeling and Computation of Boundary-Layer Flows*. Horizons Publishing Inc., 2. edition.
- [Durbin and Pettersson-Reif, 2011] Durbin, P. and Pettersson-Reif, B. (2011). *Statistical Theory and Modeling for Turbulent Flow*. John Wiley & Sons, Ltd, 2. edition.
- [Faltinsen, 1990] Faltinsen, O. (1990). *Sea Loads On Ships And Offshore Structures*. Cambridge University Press.
- [Fredheim, 2005] Fredheim, A. (2005). *Current forces on net structures*. PhD thesis, Department of Marine Technology, Norwegian University of Science and Technology.
- [Lader and Enerhaug, 2005] Lader, P. and Enerhaug, B. (2005). Experimental investigation of forces and geometry of a net cage in uniform flow. *IEEE Journal of oceanic engineering*, 30(1).

- [Lader et al., 2007] Lader, P., Olsen, A., Jensen, A., Sveen, J., Fredheim, A., and B., E. (2007). Experimental investigation of the interaction between waves and net structures-damping mechanism. *Ocean Engineering*, 30:251–270.
- [Li et al., 2013] Li, L., Fu, S., Xu, Y., Wang, J., and Yang, J. (2013). Dynamic responses of floating fish cage in waves and current. *Ocean Engineering*, 72:297–303.
- [Lien and Volent, 2012] Lien, A. and Volent, Z. (2012). Deformasjon av not og per-maskjørt og krefter på fortyøning. Technical report, Sintef.
- [Løland, 1991] Løland, G. (1991). *Current forces on and flow through fish arms*. PhD thesis, Department of Marine Technology, Norwegian University of Science and Technology.
- [Løland et al., 1988] Løland, G., Rudi, H., and Aarsnes, J. (1988). Teori for beregning av nøter, krefter og gjennomstrømning på enkeltpaneler og merdsystem. Technical report, Marintek SINTEF-Gruppen.
- [Moe et al., 2010] Moe, H., Fredheim, A., and Hopperstad, O. (2010). Structural analysis of aquaculture net cages in current. *Journal of Fluids and Structures*, 26:503–516.
- [Næs et al., 2012] Næs, M., Hauch, P., and Mathisen, R. (2012). Bruk av "luseskjørt for å redusere påslag av lakselus *Lepeophtheirus salmonis* (krøyer) på oppdrettslaks. Technical report, NCE-Aquaculture.
- [Patursson et al., 2006] Patursson, Ø., Swift, M., Baldwin, K., Tsukrov, I., and Simonsen, K., editors (2006). *Modeling flow through and around a net panel using computational fluid dynamics*. Proceedings of the OCEAN 2006 IEEE Xplore.
- [Rundtop and Lien, 2013] Rundtop, P. and Lien, A. (2013). Krefter og deformasjon av skjørt i fhsim. Technical report, Sintef.
- [Shim et al., 2009] Shim, K., Klebert, P., and Fredheim, A., editors (2009). *Numerical investigation of the flow through and around a net cage*. Proceedings of the ASME 2009 28st International Conference on Ocean, Offshore and Arctic Engineering.
- [Sumer and Fredsøe, 2006] Sumer, B. and Fredsøe, J. (2006). *Hydrodynamics Around Cylindrical Structures*, volume 26. World Scientific.
- [Tsukrov et al., 2003] Tsukrov, I., Eroshkin, O., Fredriksson, D., Robinson Swift, M., and Celikkol, B. (2003). Finite element modeling of net panels using a consistent net element. *Ocean Engineering*, 30:251–270.
- [White, 2006] White, F. (2006). *Viscous fluid flow*. McGraw-Hill, 3. edition.

# Appendix A

## Simulation results

Drag force [N]						
Full configuration			AquaSim			
Current velocity [m/s]	Experiment	FhSim	Sn = 1	Sn = 0,9	Sn = 0,8	
0,05	7,848	14,1	23,37	22,32	20,757	
0,1	19,42	35	51,52	41,39	31,295	
0,15	33,05	58	69,91	55,415	40,854	
0,2	42,86	77,5	91,77	61,545	48,291	

Current velocity [m/s]	Sn = 0,7	Sn = 0,6
0,05	14,61	8,89
0,1	23	18,46
0,15	33,55	28,61
0,2	43,57	38,59

Skirt only						
Current velocity [m/s]	Experiment	FhSim	Sn = 1	Sn = 0,9	Sn = 0,8	
0,05	3,8259	12,00	20	19,2	17,5	
0,1	10,0062	27,00	34	42,4	27,7	
0,15	19,3257	43,00	50	46,36	36,5	
0,2	26,8794	55,00	65	52,4	43,1	

Current velocity [m/s]	Sn = 0,7	Sn = 0,6
0,05	11,9	6,9
0,1	17,4	11,8
0,15	25	19,7
0,2	31,25	26,3

Figure A.1: Results from drag force [N] simulation in AquaSim, presented as numbers.

<b>Deformation front [%]</b>					
Full configuration			AquaSim		
Current velocity [m/s]	Experiment	FhSim	Sn = 1	Sn = 0,9	Sn = 0,8
0,05	9,1	28,37	27,29	24,60	12,91
0,1	42,1	58,68	60,98	58,71	50,61
0,15	61,4	75,48	77,10	75,78	68,84
0,2	83,5	79,96	84,64	84,34	78,69

Current velocity [m/s]	Sn = 0,7	Sn = 0,6
0,05	11,83	2,53
0,1	48,43	32,97
0,15	70,75	59,90
0,2	81,02	73,70

<b>Skirt only</b>					
Current velocity [m/s]	Experiment	FhSim	Sn = 0,9	Sn = 0,8	Sn = 0,7
0,05	9,1	28,37	50	45,33	48,34
0,1	42,1	58,68	77,61	74,14	72,87
0,15	61,4	75,48	88,45	86,12	82,65
0,2	83,5	79,06	93,66	91,34	87,94

Current velocity [m/s]	Sn = 0,6
0,05	33,22
0,1	61,99
0,15	74,55
0,2	81,41

Figure A.2: Results from deformation simulation at the fore side of the skirt, presented as percent of initial skirt depth.

Deformation aft [%]		AquaSim				
Full configuration		Experiment	FhSim	Sn = 1	Sn = 0,9	Sn = 0,8
Current velocity [m/s]						
0,05	0,8	25,62	16,66	14,51	9,31	
0,1	0,8	55,92	83,30	79,49	26,83	
0,15	11,8	74,1	92,87	88,55	53,32	
0,2	33,9	79,34	96,83	94,43	73,46	

Current velocity [m/s]	Sn = 0,7	Sn = 0,6
0,05	5,23	0,36
0,1	5,61	4,61
0,15	27,01	23,82
0,2	56,27	51,63

Skirt only		AquaSim			
Current velocity [m/s]	Experiment	FhSim	Sn = 0,9	Sn = 0,8	Sn = 0,7
0,05	0,83	25,62	25,74	20,39	12,81
0,1	0,83	55,92	95,38	26,92	0,03
0,15	11,85	74,10	94,56	48,46	0,08
0,2	33,88	79,34	97,22	62,27	0,51

Current velocity [m/s]	Sn = 0,6
0,05	8,08
0,1	0,28
0,15	3,20
0,2	12,82

Figure A.3: Results from deformation simulation at the fore side of the skirt, presented as percent of initial skirt depth.

<b>Drag force [N]</b>			
<b>Net cage without Permaskirt</b>			
Current velocity [m/s]	Experiment	FhSim	AquaSim
0,05	4,21	3,5	3,9
0,1	12,06	12	13,1
0,15	21,77	22	24,9
0,2	31,39	36	39,4

Figure A.4: Drag force values for net cage only. The net cage had a solidity of 0.21.